

**AGGREGATE SUITABILITY STUDIES OF HABIB RAHI
FORMATION EXPOSED AT GULKI HILLS, ZINDAPIR ANTICLINE,
DERA GHAZI KHAN, PAKISTAN**



DANISH FAROOQ

02112113007

M.PHIL GEOLOGY

2021-2023

DEPARTMENT OF EARTH SCIENCES

QUAID-I-AZAM UNIVERSITY

ISLAMABAD, PAKISTAN

CERTIFICATE

It is certified that **Mr. Danish Farooq, S/o Muhammad Farooq (Registration No. 02112113007)**, carried out the work contained in this dissertation under my supervision and accepted it in its present form by Department of Earth Sciences as satisfying the requirements for the award of **M.Phil Degree in Geology**.

RECOMMENDED BY

Dr. Abbas Ali Naseem

Associate Professor/Supervisor

Dr.

External Examiner

Prof. Dr. Mumtaz M. Shah

Chairperson

Department of Earth Sciences

Quiad-i-Azam University

Islamabad

Acknowledgement

To my mentors and advisors:

The author would like to offer heartfelt thanks to **Associate Professor Dr. Abbas Ali Naseem** your guidance, expertise, and commitment to my intellectual growth have shaped the foundation of this thesis. I am deeply grateful for the knowledge you have imparted and the valuable insights you have provided. This work is dedicated to you, as a testament to the impact of your mentorship on my academic journey.

To my loving family:

Without your unwavering support, encouragement, and sacrifices, this journey would have been impossible. Your belief in me has been my driving force, and your love has been my constant inspiration. This dissertation is dedicated to each one of you, for your boundless faith in my dreams and your enduring presence throughout this challenging endeavor.

To my friends:

Special thanks to **Zubair Ahmad, Fayaz Rehman, and Muzammil Usmani** for standing by me during the long hours of research, the moments of doubt, and the celebrations of small victories. . This dissertation is dedicated to our shared memories and the bonds we've forged along the way.

To all those who have contributed to my academic and personal growth, this dissertation is a culmination of the collective support, encouragement, and inspiration. I have received from so many people along the way. I extend my heartfelt dedication to all of you who have played a part in my academic journey.

With deep gratitude and appreciation,

Danish Farooq

September 2023

Abstract

The construction industry has a significant positive impact on the socioeconomic development of a country. The demand for building supplies in Pakistan has significantly increased since the China-Pakistan Economic Corridor (CPEC) project got underway since 2015. The N-S trends of Zindapir anticline is doubly plunging anticline located in the easternmost part of the Sulaiman Range. In this context, a comprehensive evaluation was undertaken to investigate the suitability of limestone deposits from the Habib Rahi Formation as a potential source of coarse aggregate, for construction projects. In this study, the Limestone of Habib Rahi Formation from Zindapir Anticline has been used to examine its geochemistry, petrography, and physical-mechanical characteristics for usage of coarse aggregate. In petrographic terms, the Habib Rahi Formation aligns with the classification of mudstone and wackestone as per the Dunham classification scheme. It is predominantly composed of calcite and bioclast, which serve as the major constituents within a fine-grained micrite. The Limestone of Habib Rahi Formation was investigated through geochemistry (PXRF), the major mineral phases include CaO (48.7%), SiO₂ (5.6%), Al₂O₃ (1.2%), Fe₂O₃ (1.2%), K₂O (0.2%), and TiO₂ (0.1%). Alkali-silica reaction in accordance with (ASTM C 1260) also reveal that the limestone of the Habib Rahi Formation has an expansion of less than (0.1%) indicating a safe nature. The geotechnical tests were performed in accordance with the requirements of the American Standards for Testing Materials (ASTM). The results of numerous tests for coarse aggregates, including those for specific gravity, and water absorption test (2.3%), flakiness and elongation test (5.9%), loss angeles abrasion test (28.6%), soundness test (5.7%), aggregate impact value test (25.1%), aggregate crushing value test (25.4%), unit weight test (1.29%), and coating and striping (>90%). Cumulatively, the findings derived from petrographic, geochemical, and geotechnical analyses are integrated to indicate the potential of the Habib Rahi Formation within the Zindapir Anticline as a prospective source of coarse aggregates for construction projects. Utilizing local resources like the Limestone of the Habib Rahi Formation in the progressing construction sector can significantly enhance sustainable practices, promoting both infrastructure development and economic growth.

Table of Contents

Abstract.....	iv
List of Figures.....	viii
List of Tables	xi
Chapter #1	1
Introduction.....	1
1.1 Location of study area	3
1.2 Aims and Objectives	4
1.3 Previous Work.....	4
Chapter #2	7
Geological Settings	7
2.1 Local Geology	9
2.2 Stratigraphy of the Area	10
2.2.1 Kirthar Formation.....	12
2.2.1.1 Drazinda Formation	12
2.2.1.2 Pirkoh Formation.....	12
2.2.1.3 Domanda Formation.....	13
2.2.1.4 Habib Rahi Formation	13
2.2.2 Ghazij Formation.....	13
2.2.2.1 Baska Formation.....	13
2.2.2.2 Drug Formation	14
2.2.2.3 Shaheed Ghat Formation	14
2.2.2.4 Dungan Formation.....	14
2.2.2.6 Khadro Formation	15
2.2.2.7 Pab Formation.....	15
2.2.2.8 Fort Munro Formation.....	15
2.2.2.9 Mughal Kot Formation.....	16
CHAPTER #3.....	17
Methodology	17
3.1 Introduction.....	17
3.2 Fieldwork.....	17

3.3 Laboratory work	18
3.3.1 Petrographic analysis	18
3.3.2 Geochemical test	19
3.3.2.1 XRF	19
3.3.2.2 ASR ASTM C-1260	19
3.3.3 Physical test	20
3.3.5 Mechanical test	24
3.3.6 Bituminous test	26
Petrography and Geochemistry	28
4.1 Introduction	28
4.2 Sample Collection	28
4.3 Thin Section Preparation	29
4.4 Petrographic details	29
4.5 Geochemical test	36
4.5.1 Introduction	36
4.6 Alkali-silica reaction	41
Chapter #5	43
Geotechnical Analysis	43
5.1 Physical Test	43
5.1.1 Sieve Analysis for Coarse Aggregate	43
5.1.2 Specific Gravity and Water Absorption	44
5.1.3 Particles shape (Flakiness and elongation)	45
5.2 Durability Test	49
5.2.1 Loss Angeles Test	49
5.2.2 Soundness Test	51
5.3 Mechanical test	53
5.3.1 Aggregate Impact Value	53
5.3.2 Aggregate Crushing Value	55
5.3.3 Unit Weight	57
5.4 Bituminous test	60
5.4.1 Coating and Striping	60

CHAPTER #6	62
Results, Conclusion and Recommendation	62
6.1 Results	62
6.2 Conclusion and Recommendation	63
References	65
APPENDIX	72
Formula	72
1. Specific gravity and water absorption	72
2. Loss Angeles Abrasion Value (LAAV)	72
3. Aggregate impact value	72
4. Aggregate Crushing value (ACU)	73

List of Figures

Figure 1.1	Landsat image showing the study area of Zindapir Anticline (Google Earth).....	4
Figure 1.2	Flow chart of the research methodology.....	6
Figure 2.1	Tectonic elements of Pakistan and neighboring region (Modified after Kazmi & Jan 1997).....	8
Figure 2.2	Schematic cross-sections across Sulaiman Depression, Zindapir Anticline and Bharti Syncline showing structural pattern associated with transpressional regime (after Ali. et.al, 1995).....	9
Figure 2.3	Generalized stratigraphic chart of Zindapir Anticline.....	11
Figure 3.1	Field photographs of Habib Rahi Formation (A) Road cut section (B, C) benthic foraminifera (D) Chert Bed.....	18
Figure 3.2	ASR test in progress at PCSIR Peshawar.....	19
Figure 3.3	Specific Gravity test in progress at SABHAN Geotechnical Laboratory.....	20
Figure 3.4	Sieve Analysis in progress at SABHAN Geotechnical Laboratory.....	21
Figure 3.5	Loss Angeles abrasion test in progress at SABHAN Geotechnical Laboratory.....	23
Figure 3.6	Soundness test in progress at SABHAN Geotechnical Laboratory.....	24
Figure 3.7	Aggregate Impact Value machine at SABHAN Geotechnical Laboratory.....	25
Figure 3.8	Unite weight instruments at SABHAN geotechnical.....	26

	laboratory.....	
Figure 4.1	Photomicrograph of Habib Rahi Limestone (HR-1) showing Bioclast (Bc), and Pyrite leaching (Pl).....	31
Figure 4.2	Photomicrograph of Habib Rahi Limestone (HR-1) showing Bioclast (Bc), and Pyrite leaching (Pl).....	31
Figure 4.3	Photomicrograph of Habib Rahi Limestone (HR-2) showing Micrite (Mc), and Bioclast (Bc).....	32
Figure 4.4	Photomicrograph of Habib Rahi Limestone (HR-2) showing Fracture (Fr), and Pyrite leaching (Pl).....	32
Figure 4.5	Photomicrograph of Habib Rahi Limestone (HR-3) showing Bioclast (Bc), Micrite (Mc).....	33
Figure 4.6	Photomicrograph of Habib Rahi Limestone (HR-3) showing Bioclast (Bc), Micrite (Mc), and Pyrite leaching (Pl).....	33
Figure 4.7	Photomicrograph of Habib Rahi Limestone (HR-4) showing Micrite (Mc), and Bioclast (Bc).....	34
Figure 4.8	Photomicrograph of Habib Rahi Limestone (HR-4) showing Calcite vein (Cv), and Bioclast (Bc).....	34
Figure 4.9	Photomicrograph of Habib Rahi Limestone (HR-5) showing Chert grains (Ch), and Micrite (Mc).....	35
Figure 4.10	Photomicrograph of Habib Rahi Limestone (HR-5) showing Chert grains (Ch), and Pyrite leaching (Pl).	35
Figure 4.11	Graphical comparison of CaO in the collected rock samples of Habib Rahi Formation.	38
Figure 4.12	Graphical comparison of SiO ₂ in the collected rock samples of Habib Rahi Formation	38
Figure 4.13	Graphical comparison Fe ₂ O ₃ in the collected rock samples of Habib Rahi Formation.	39
Figure 4.14	Graphical comparison of Al ₂ O ₃ in the collected rock samples of Habib	39

	Rahi Formation.	
Figure 4.15	Graphical comparison of K_2O in the collected rock samples of Habib Rahi Formation.	40
Figure 4.16	Graphical comparison of TiO_2 in the collected rock samples of Habib Rahi Formation.	40
Figure 5.1	Graphical representation of Specific Gravity and Water absorption.	45
Figure 5.2	Graphical representation of Flakiness and Elongation index.	48
Figure 5.3	Graphical representation of Loss in weight samples.	50
Figure 5.4	Graphical representation of soundness test.	53
Figure 5.5	Graphical representation of Aggregate Impact Value.	55
Figure 5.6	Graphical representation of Crushing Value.	57
Figure 5.7	Graphical representation of unit weight.	59
Figure 5.8	Graphical representation of bitumen test	61

List of Tables

Table 4.1	Model composition of Habib Rahi Formation at Zindapir anticline.	30
Table 4.2	Geochemical analysis of various samples of Habib Rahi limestone.....	37
Table 5.1	Tabular presentation of sieve analysis of coarse aggregate.....	44
Table 5.2	Result of water absorption specific gravity and porosity of different rock samples.....	45
Table 5.3	Flakiness and elongation test values for the aggregate of Habib Rahi formation	47-48
Table 5.4	Loss Angeles test for Habib Rahi formation.....	50
Table 5.5	Gradation of aggregate and their weights for soundness test of Habib Rahi formation.....	52
Table 5.6	Impact value test results for the limestone sample of Habib Rahi formation.....	55
Table 5.7	Crushing value test for the aggregate of Habib Rahi formation.....	56
Table 5.8	Unit weight result for the Habib Rahi formation.	59
Table 5.9	Bitumen test for the aggregate of Habib Rahi formation	61

Chapter #1

Introduction

Introduction

The most often used natural aggregate for the construction industry in Pakistan is limestone. The main component of the various rocks that revealed in Himalayan mountain ranges of northern as well as southern Pakistan are limestone deposits. The various formations, such as the Samana Suk Formation, Margalla Hill Limestone, Kohat Formation, Wargal Limestone, Kawagarh Formation, Lockhart Formation, Shekhai Formation, Lockart Limestone, and Sakesar Limestone, play a vital role in meeting the construction demands of the nation. Understanding the geological characteristics and distribution of these formations is crucial for sustainable sourcing and utilization of limestone aggregates in Pakistan's construction industry. (Nizami, 2008; Rehman, 2009, 2017; Rehman et al., 2016; Ahsan et al., 2012; Shah, 2009).

The limestone deposits are widely exposed in various regions of Pakistan and are easily usable for a variety of construction projects. Precambrian to Eocene in age are these limestone formations. The construction industry would gain advantages from an extensive examination of these limestone formations using various physico-mechanical suitability studies in various regions of the country. Limestone is a common raw material used in a variety of industries, particularly the cement and construction sectors.

The economic development of a nation is greatly influenced by the construction industry. Since the China-Pakistan Economic Corridor (CPEC) project began in 2015, the requirement for building supplies in Pakistan has dramatically expanded. It is crucial to take into account new choices for construction materials in the context of CPEC projects. One of the most often used building materials is limestone. The mineral calcite (CaCO_3) comprises up the majority of this remarkable sedimentary rock. It is important to carry out a prospective study for the examination of new resources given the projection of a considerable development in the demand for building materials and construction projects.

Igneous, sedimentary, and metamorphic rocks are potential Geologic resources (Roberts, 1996). Amongst these rocks, the crushed forms like cobbles, pebbles, and gravels, mainly of the sedimentary rocks, share the production of the main products for construction material and aggregates. On the other hand, depending on their suitability and transportation costs, igneous and metamorphic rocks were also

be used as aggregate. Aggregates are used for stiff pavements and infrastructure (Somro et al., 2016); (Sanaullah et al., 2017); (Varghese, 2015).

Limestone serves as the primary raw material for concrete. It is essential for the development of the modern economy since it is used in the construction of highways, structures, bridges, and tunnel walls as an aggregate material obtained from quarrying and crushing activities. (Galetakis et al., 2012).

In concrete structures, roadways, asphalt bases and pavements, and other construction projects, aggregates are frequently natural or crushed rock. They generally consist of weathered or blasted pieces of fragmented rock. Physical, mechanical, and geochemical characteristics, such as particle size, lithology, appearance, strength, resistance to abrasion, and soundness, are typically used to classify these materials. Gravel, sand, and mud deposits are the main components of natural aggregates. These materials were deposited by a variety of natural processes, including water, wind, and glaciers. The most often utilized and widely accessible type of rock for this purpose is limestone, which is also the best natural source of crushed aggregates.

The presence and quantity of reactive elements that may result in structural damage to the concrete and asphalt constructions in which these rock aggregates are utilized are identified through microscopic petrographic analyses of rock aggregates (Berube and Fournier, 1993; Gilbert, 1995). In order to estimate different reactions before employing aggregates in concrete and asphalt operations, petrographic examinations of the aggregates are absolutely essential (Desai, 2010).

The physico mechanical properties of a rock is evaluated to identify their feasibility for use as rock aggregates in different construction projects. The aggregates used in a construction project must be resistant to abrasion and disintegration that is compacted with rollers and traffic loading (Wiesma, 1990; Wiersma, M. 1990). The rock aggregates, which are not tough enough and abrasion resistant may cause failures in the structure.

To determine whether aggregate is suitable for any construction use, a range of technical tests must be conducted, such as Specific Gravity and Water Absorption test (WA); Soundness (SD); Crushing Value (CV); Aggregate Impact Values (AIV); Unit weight (UW); Flakiness index (FI); Elongation index (EI); Los Angeles Abrasion value (LAAV); Coating and striping (CS) (Khanlari; Naseri, 2018).

The chemical composition of limestone is a reflection of its mineral composition. For that purpose, we adopt some geochemical investigation by XRF, which is a commonly adopted method in experimental studies that analyzes major and trace elements and oxides quickly and precisely.

Moreover, alkali-rich limestone is considered unsuitable for the cement industry because it affects concrete. These alkalis degrade cement quality causing Alkali-Silica Reactions which result in the formation of a swelling gel (Ertek, 2005; Insley, 1950). Silica gel forms then silica in the aggregates reacts to the alkali cement, in presence of water. According to (Ferraris; Ferraris 1995), Osmotic pressure caused by the silica gel weakens the link between cement and aggregate, leading to cracks in the buildings. For this reason, the alkali silica reaction test (ASTM, C-1260) is the standard method that is followed to investigate limestone units.

This project is thus designed to evaluate the physico-mechanical and geochemical investigations regarding aggregate potential of the Eocene Habib Rahi limestone exposed in Zindapir Anticline, Central Indus Basin, Pakistan.

1.1 Location of study area

The Zindapir Anticline is a part of the Sulaiman Fold Belt, which is exposed North-South trending of South Punjab and Baluchistan. The location of study area is situated on the Eastern flank of Zindapir Anticline, which is situated in Gulki village (Lat.30°42'51"N;Long.70°27'27"E) located near Tunsu Shareef, approximately 30 kilometers away from district Dera Ghazi Khan, Punjab, Pakistan.



Fig.1.1 Landsat image showing the study area of the Zindapir Anticline (Google Earth).

1.2 Aims and Objectives

The current research work is to evaluate Eocene limestone that are exposed in Zindapir Anticline Central Indus Basin in terms of their suitability studies for construction projects in rock aggregate potential. The aim will be achieved through the following objectives:

1. To carry out detailed petrographic analysis of the samples in thin sections collected from Eocene Carbonate Habib Rahi Limestone exposed in Zindapir Anticline Central Indus Basin.
2. To determine the physico-mechanical properties of Habib Rahi Limestone exposed in Zindapir Anticline, Central Indus Basin, Pakistan.
3. To evaluate the geochemical analysis of collected samples through XRF for elemental analysis, and the Alkali-Silica Reaction (ASR) tests are conducted to determine whether concrete buildings are susceptible to the Alkali-Silica Reaction.

1.3 Previous Work

Researchers like (R.S. Boynton, 1980; Oats, 1998) previously investigated the industrial usage of limestone. (Hussain et al., 1989) conducted a comprehensive study on the petrological and commercial applications of the Nizampur limestone in Khyber Pakhtunkhwa, Pakistan. The study's findings suggested that the limestone in the study area is suitable for usage in the cement industry. Similar to this, (Bilqees, and Shah, 2007) investigated limestone deposits in the Kohat territory for industrial uses and

recommended its utilisation in the cement market. The limestone from the Nizampur territory has been examined by (Jan et al., 2009) who recommended utilizing it in the paper, glass, and cement industry sectors. The Abbottabad limestone has been examined and determined to be appropriate for usage in several types of industries, including cement (Bilqees et al., 2012). The Samana Suk Formation, Kawagarh Formation, Lockhart Limestone, and Margalla Hill Limestone of the Abbottabad area have also been qualified for cement as well as construction usage (Bilqees et al., 2015). In the same way, researchers (Malahat et al., 2018) and (Rehman et al., 2018) investigated the suitability of limestone as an aggregate suitability in Khyber Pakhtunkhwa. However, there are still significant reserves of limestone that haven't been properly assessed. Thus, the current research is aimed as a continuation of the earlier research in order to evaluate the limestone resources that have not yet been explored and tested of the Zindapir Anticline Central Indus Basin, which has several deposits of limestone.

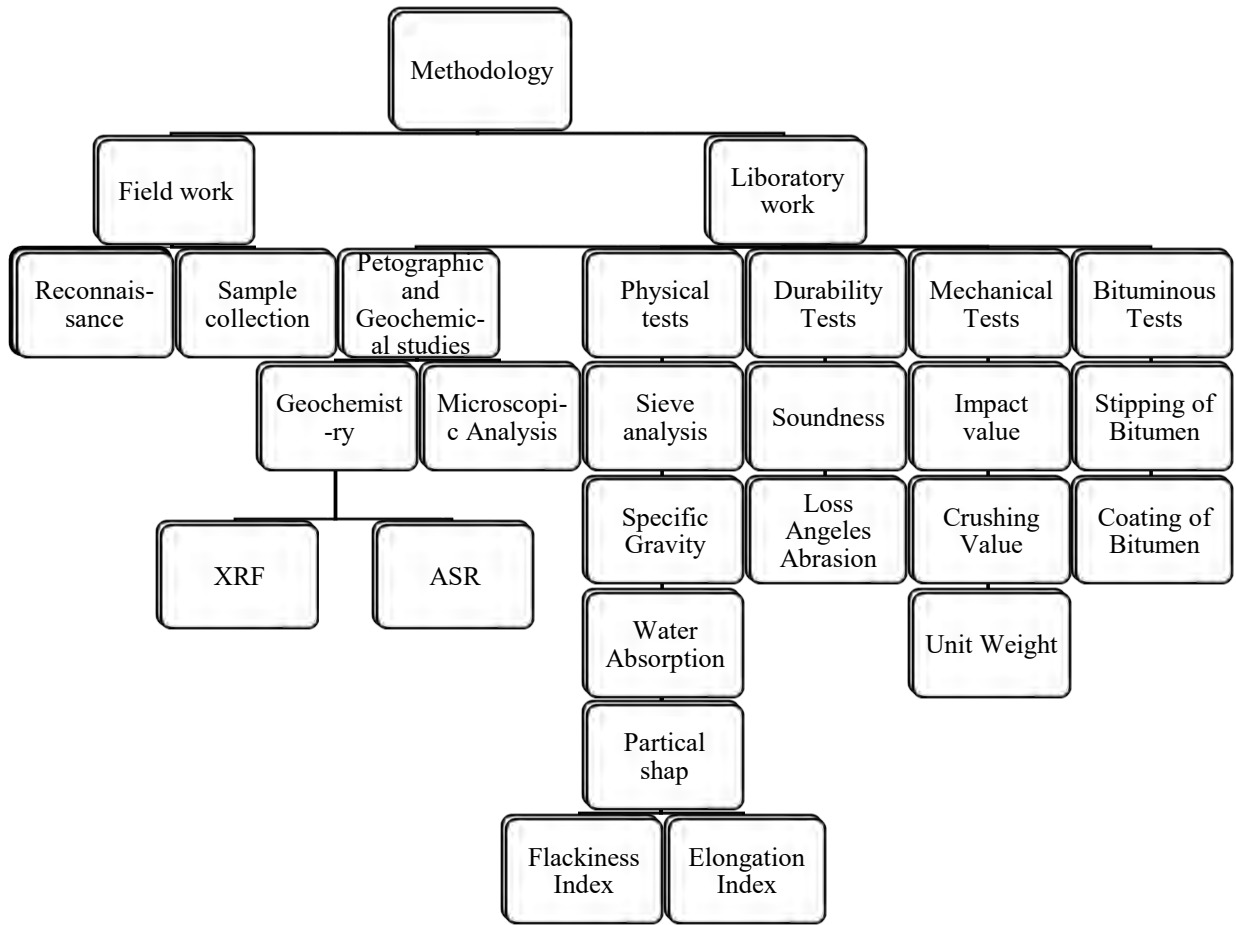


Figure 1.2 Flow chart of the research methodology.

Chapter #2

Geological Settings

Geological Settings

The Gondwanaland Super Continent's intracratonic rifting in the late Protozoic, followed by the Permian-Triassic rift event, marked the start of the Indus Basin's tectonic episodes. The detachment of the Indian plate with the Afghan, African, and Seychelles cratonic aspects during the last phase of the Mesozoic rifting caused those cratonic elements to start drifting north, which led to a massive plate convergence with the Eurasian mass throughout the Cenozoic era (currently ongoing) (Kemal et al., 1991). The Indo-Pakistan Plate was splits into various basement blocks which are Kirthar Basement Fault, the Sulaiman Basement Fault, and the Jhelum Basement Fault, which all opened as a result of the anticlockwise rotation caused on by the oblique collision of the Indo-Pakistan Plate with the Eurasian Plates. Different tectonic patterns were created on each individual basement block as a result of these blocks shifting during the impact (Bannert and Raza, 1992). Widespread deposits during Infra Cambrian-Eocene source and reservoir rocks of carbonate as well as clastics origin was caused by the different geodynamic conditions throughout geological time in the Indus Basin. These conditions have primarily been described by Khan et al., 1986; Malik et al., 1988; Raza et al., 1989; and Raza et al., 1990 According to (Ali et al., 1995) the formation of various structural and stratigraphic traps associated with transpressional-transtensional regimes, rift inverted extensional episodes, salt tectonics discontinuities, and clastic and carbonate units/facies of low-high stand system tracts (Kemal, 1988; Raza et al., 1989; Ahmed and Ali, 1991; Bannert et al., 1992; Ali et al., 1995; Ahmad et al., 2004; Iqbal et al., 2008; Afzal et al., 2009). Due to left and right lateral transpressional regimes associated with wrench tectonics in the east and west, respectively, the Sulaiman Fold Belt developed in the Late Tertiary. Positive flower structure, thrust and sub-thrust structural patterns in the subsurface are signs of wrench-related thick-skinned tectonic features on the surface. Left-lateral en-echelon folds and associated thrust faults are found in the east, while right-lateral en-echelon folds and related fault systems are found in the west. In the Safed Koh Range, which is found in the eastern part of the Sulaiman Fold Belt, the left-lateral wrench regime produced a number of north-south en echelon folds are oriented with hydrocarbon pools associated with positive floral structures (Ali et al., 1995). In the eastern part of the Sulaiman Fold Belt, positive floral structures connected to wrenches have also been hypothesized by (Bannert et al., 1995), (Iqbal, 2004, PhD), (Iqbal et al., 2008), and (Peresson and Daud, 2009). (Iqbal et al., 2008) predicted that the majority of underfilled structures and also the absence of hydrocarbon formation in some of the structures are

caused by the Sulaiman Fold Belt's young age (Late Tertiary) and quick uplift rate, and they viewed the Sulaiman Foredeep as a hydrocarbon a kitchen that charged the anticlines.

However, for the Sulaiman Fold Belt, the passive roof duplex model related to thin-skinned tectonics has been proposed by (Banks and Warburton, 1986) and (Humayon et al., 1991). The exposed rocks in the Sulaiman Fold Belt believed to date from the Triassic to the Tertiary, according to Rasa et al. (1989), Hunting Survey Corporation (1960), Baker and Jackson (1964), Kazmi and Jan (1997), Shah(2009), and Bannert et al. (1989). Zindapir Anticlinorium reservoirs have been discovered in the carbonates of the Chiltan Formations (Jurassic), Lower Goru (Early Cretaceous), and Pab Formations (Late Cretaceous), Ranikot Sands, and Dunghun Limestone (Paleocene).

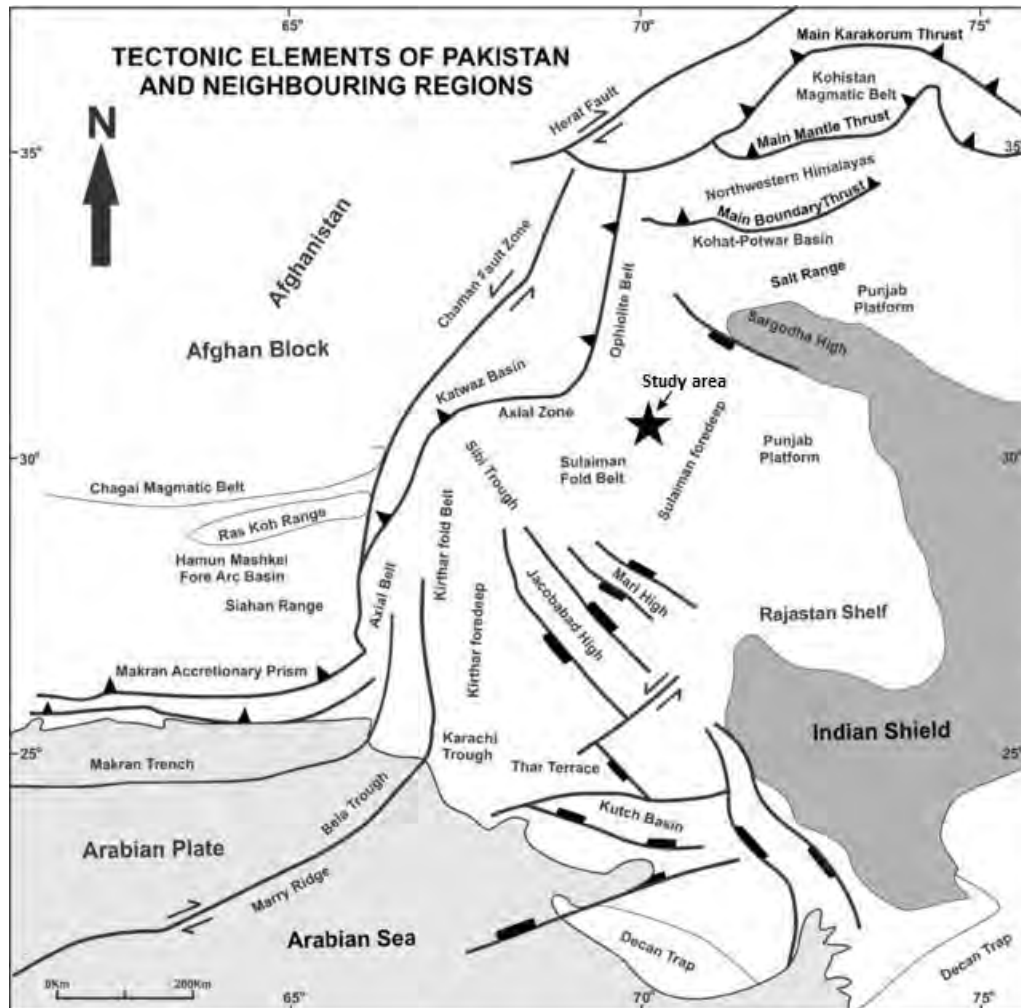


Figure 2.1: Tectonic elements of Pakistan and neighboring regions (Modified after Kazmi & Jan, 1997).

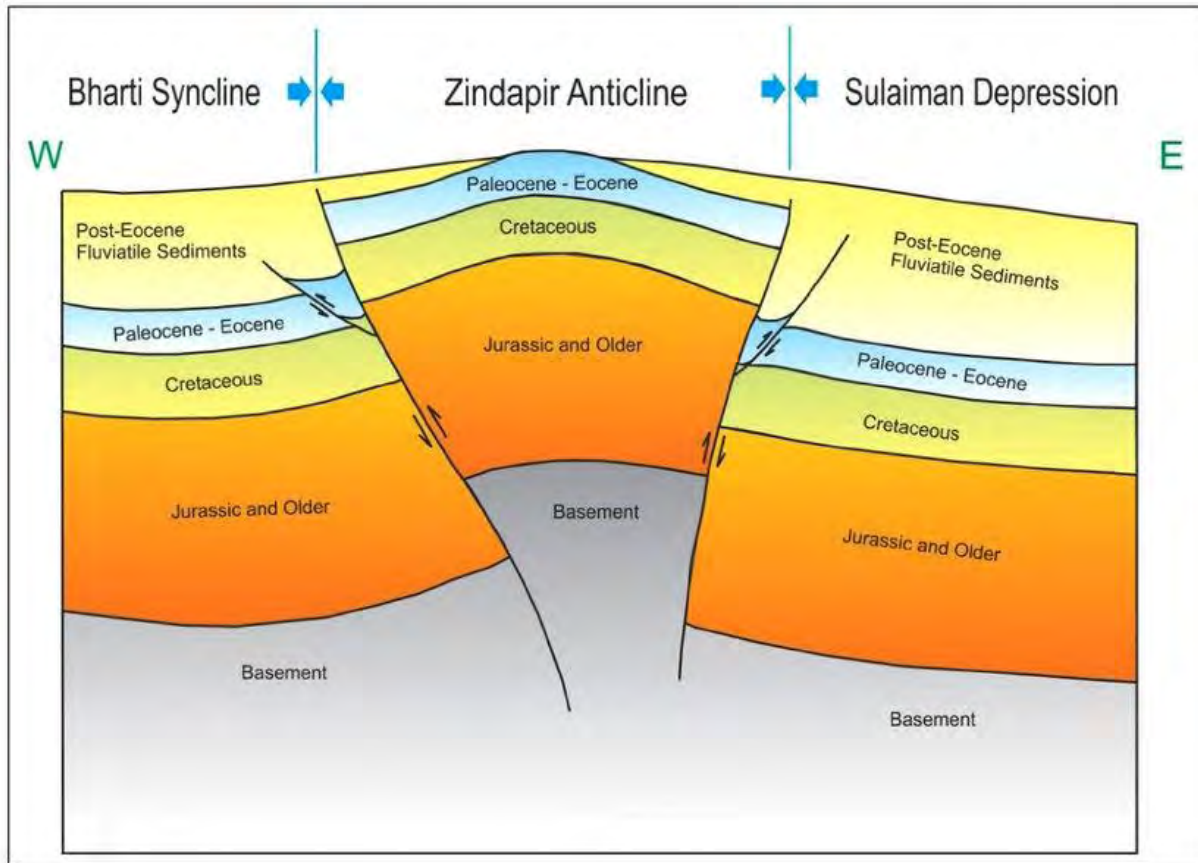


Figure 2.2 Schematic cross-sections across Sulaiman Depression, Zindapir Anticline, and Bharti Syncline showing structural patterns associated with transpressional regime (after Ali. et.al, 1995).

2.1 Local Geology

In the most eastern section of the Sulaiman Range is found a doubly plunging anticline known as the Zindapir Anticline. The overall trending of this range is north to south. The Early Paleocene Rakhi Gaj Sandstone and Shale, which is the main formation exposed in Zindapir Ziarat Gorge, is topped by the huge and thick limestone of the Late Paleocene Dungan Formation. The anticlinal axis' summits, which extend more than 10 km north to south, are formed by the Dungan Limestone. This limestone is also being used for D.G. Khan Cement industry. Due to their high affinity for erosion, the Early Eocene Shaheed Ghat shales are found on the limbs and plunging areas (Mureed Hussain Khosa et al., 2016).

The Early Eocene Drug rubbly limestone, Baska gypsum, and Drazinda shale of the Chamalang (Ghazij) Group, the Middle Eocene Habib Rahi limestone, Domanda shale, Pirkoh marl-limestone, and Drazinda shale of the Kahan Group, and the Oligocene Chitarwata (ferruginous sandstone (greenish grey sandstone with some red muds) and Pliocene Chaudhwan (alternated sandstone and maroon muds) of

Vihowa Group and Pleistocene Dada (conglomerate) and Holocene Sakhi Sarwar (clays, sandstone and conglomerates) of Sakhi Sarwar Group. After the exposures of the Sakhi Sarwar Formation, the eastern limb is mostly covered by thick alluvium with some eolian deposits. The western limb shares the Baghal Chur-Barthi-Fazla Kach syncline. The Eocene and post Eocene rocks plunge in the south at Dalana, Sakhi Sarwar areas, etc., and in the north at Sanghar, Satta Post, Litra, and Vihowa areas. (Mureed Hussain khosa et al., 2016).

2.2 Stratigraphy of the Area

The Mesozoic in Sulaiman and Kirthar is very similar to one another, but the Tertiary is different, because the source in Kirthar's southern region was an Indian shield, while the source in Sulaiman and Kirthar's northernmost region was a hinterland similar to Afghanistan.

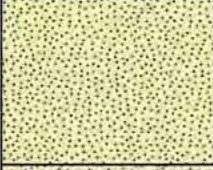





Age		Formation	Description	Thickness	Lithology	
Quaternary	Holocene	Recent Deposits	Alluvium, Meander Belt, Active Flood and Dune Sand Deposits	2000m		
		Sub-recent Deposits	Flood plain, Sub Piedmont, Piedmont, Alluvial Fan and Terrace Gravel Deposits			
	Pleistocene	Dada Conglomerate	Light brownish grey, massive conglomerate, boulders, cobbles, pebbles of sandstone and limestone	9m		
Neogene	Pliocene	Siwalik Group	Chaudhwan Formation	+1422m		
			Litra Formation	Sandstone with minor clay		+2002m
			Vihowa Formation	Claystone with sandstone		+975m
Paleogene	Oligocene Miocene	Chitarwata Formation		Sandstone with siltstone	320m	
		Drazinda Formation		Shale with siltstone	583m	
	Eocene	Pirkoh Formation		Limestone	19m	
		Domana Formation		Claystone/shale	460m	
		Habib Rahi Formation		Limestone	74m	
		Baska Formation		Shale and limestone	277m	
		Drug Formation		Limestone	345m	
		Shaheed Ghat Formation		Shale with intercalated siltstone and limestone	1870m	
	Paleocene	Dungan Formation		Limestone	211m	
Rakhi Gaj Formation		Shale intercalated sandstone	357m			

Fig 2.3 Generalized stratigraphic chart of the Zindapir Anticline

2.2.1 Kirthar Formation

The term 'Kirthar' is recognized by (Kadri, 1995). In the Sulaiman Range and the Central Indus Basin, the sediments as defined were divided into four distinct Formations, namely the Drazinda, Pirkoh, Sirki/Domanda, and Habib Rabi Formation (Raza et al., 2001). The Kirthar Formation spans from the lowermost Lutetian (Middle Eocene) to uppermost Ypresian (Lower Eocene), according to (Raza et al., 2001).

2.2.1.1 Drazinda Formation

The Drazinda Formation was designated the top Formation of the Kirthar Group by (Iqbal, and Shah, 1980), although it was not recognized as such by (Raza et al., 2001). It is composed of non-calcareous shales that varying in colour that is grey to brown, and have poorly developed fossiliferous limestone interbeds that are widely exposed throughout the eastern side of the SFB and Central Indus Basin. It has an upper unconformable contact with the Chitarwata Formation in the Zindapir area and a lower transitional contact with the Pirkoh Formation. The absence of the Nari and Gaj Formation in other areas is due to an important regional unconformity. The lithology in the Zindapir region is comprised of brown and green shale/claystone, siltstone, marl, and remains of animals such as fish, cows, and whales. The Chitarwata Formation can reach a depth of 583 meters in Zindapir area.

2.2.1.2 Pirkoh Formation

The term Pirkoh was introduced by (Hemphill and Kidwai, 1973). In the Zindapir area, it is light pale yellow to brownish limestone, medium bedded in the middle unit, and massive both in the upper unit (argillaceous and marly fossiliferous) and the lower unit, comprising of abundant shallow benthic foraminifera. Its faunal assemblage includes foraminifera, bivalves, gastropods and fish remains. The type locality for the Formation is the Pirkoh structure in the Dera-Bugti region. The Pirkoh Formation is present in the south of Sulaiman province, but it is often not represented in the north due to unconformity or non-deposition (aerial photography view from satellite). The limestone consists of packstone and foraminiferal grainstone with subordinate marl beds and calcareous shales, with a discocyclinid bearing limestone bed at the base. The Pirkoh Formation in the study area displays well exposed contact with the overlying Drazinda Formation and the underlain Domanda Formation, where the nature of contact is transitional and conformable, respectively.

2.2.1.3 Domanda Formation

The 'Domanda' is introduced by (Raza et al., 2001). It is widely exposed throughout the eastern Sulaiman basin. The sediments consist of gray, often chocolate-brown, non-calcareous shales and claystone. The fauna includes foraminifera, bivalves, gastropod, and remains of sea cows and whales. It has upper conformable contact with Pirkoh Formation and attains thickness up to 460 m in Zindapir area. It has both conformable contacts underlying Habib Rahi and overlying Pirkoh Formation. The Formation contains a rich macrofaunal assemblage comprising gastropods, brachiopods, and fish remains. It is of Lutetian (Middle Eocene) age and has a depositional setting of shallow marine to brackish.

2.2.1.4 Habib Rahi Formation

The Habib Rahi Limestone formed the basal member of the Kirthar Formation as defined by (Iqbal and Shah, 1980) and was called the Platy Limestone by (Eames, 1952). It was recognized as a separate Formation by (Raza et al. 2001). The Habib Rahi Formation is Equivalent to Kohat Formation (Kadri, 1995). The Formation consist of limestone of a light gray color with shale intercalations in the lower part. The lower and upper boundaries are conformable with the underlying Ghazij and overlying Domanda Formation. It comprises light gray brownish gray limestone, argillaceous, cherty, platy, and massive at the base. The thickness of Habib Rahi Formation is up to 74m and it has age of Lutetian (Middle Eocene) and shallower, inner shelf depositional settings.

2.2.2 Ghazij Formation

In the middle Indus basin, a comprehensive study was conducted and, focusing on the petrographic and diagenetic aspects of the Ghazij Formation (Ahmed et al., 2012). Their work delved into the mineralogical composition, porosity, and permeability of the formation's sandstone intervals. This research provided insights into reservoir quality and the potential for hydrocarbon accumulation.

A sequence stratigraphic analysis of the Ghazij Formation in the Middle Indus Basin was conducted by (Yaseen et al., 2018). By examining sedimentary stacking patterns and identifying key surfaces, they reconstructed the depositional history and inferred sea-level fluctuations that influenced sediment distribution during the formation's deposition.

2.2.2.1 Baska Formation

The Baska Formation of the Ghazij Group is introduced by (Hemphill and Kidwai, 1973). It has gray color, nodular in places, argillaceous limestone, and intercalated green shale. The fauna includes

foraminifera, bivalves, gastropods, and lamellibranches. It has upper transitional contact with Habib Rahi Formation and attains thickness up to 345 m. It is restricted to the Lower Eocene (Iqbal, 1969).

2.2.2.2 Drug Formation

The Drug Formation consists of greenish gray shale and brownish gray limestone. The shale is intercalated with gypsum in the upper part. The fauna includes foraminifera and lamellibranches. In the Zindapir area, it has conformable upper contact with Habib Rahi Formation and attain a thickness of up to 356 m. The biostratigraphic age of Drug Formation is Early Eocene (Iqbal, 1969), and display an inner shelf depositional environment.

2.2.2.3 Shaheed Ghat Formation

It has dark gray, olive gray, green fissile shale intercalated with siltstone, and the gypsiferous, carbonaceous, and fossiliferous limestone is present in the lower part. The fauna includes foraminifera, gastropods, and bivalves. In Zindapir area, it has upper transitional contact with drug Formation and attain a thickness of about 1,870m. The biostratigraphy age of Drug Formation is Early Eocene (Iqbal. 1969).

2.2.2.4 Dungan Formation

It is dark gray to brown limestone, thick bedded to massive nodular, intercalated with dark bluish gray shale dominating in the southern part. The limestone conglomerate bed developed at the top of the Formation, which grades into calcareous sandstone in places. The fauna includes foraminifer gastropods, bivalves, and algae. In Zindapir area, it has upper conformable contact with the Shaheed Ghat Formation and attain thickness up to 211 m. The limestones, shales, and marls of the Dungan Formation are widely distributed throughout the Central Indus Platform Basin and conformably succeed the Upper Ranikot Formation. The Formation contains a diverse and abundant macrofossil assemblage, including bivalves and gastropods. The microfossils include melobesioidean calcareous algae and both shallow and planktonic benthonic foraminifera (Davies, 1941).

The Dungan Formation contains abundant fossils, including algae, bivalves, gastropods, and foraminifera. The foraminiferal assemblages of the Dungan Formation include dictyoconoides, discocyclina, linderina, lockhartia, operculina, nummulites, miscellanea and other shallow benthic foraminifera. It Paleocene to Early Eocene (Latif. 1964), and displays the depositional environment of typical platform limestone.

2.2.2.5 Rakhi Gaj Formation

The Rakhi Gaj Formation consists of olive-gray to dark greenish-grey shale intercalated with mostly brown to greyish red, purple, and yellowish green thin to thick bedded sandstone, iron concretions developed in shale, and also bands of grey limestone developed at places. It is fossiliferous in places, while the faunal includes foraminifera, bivalves, and gastropods. It has an upper conformable contact with the Dungan Formation and a lower conformable contact with the Khadro Formation in the Zindapir area. It attains thickness of up to 357 m. The delta of the Rakhi Gaj Formation submerged, and allowing the overlying Formation to rise in its place. It has age of middle and late Paleocene based on superposition and equivalent chronostratigraphic unit in region.

2.2.2.6 Khadro Formation

The Khadro Formation consist of dark reddish brown to gray oolitic, shelly calcareous sandstone and limestone. The limestone units are intercalated with olive gray shale. The faunal assemblages of Khadro Formation include foraminifera, bivalves, gastropods and diagnostic fossil *Cardita Beaumonti*. In Zindapir area, it has upper conformable contact with Rakhi Gaj Formation and attain thickness up to 154m.

2.2.2.7 Pab Formation

It has light gray, whitish to pinkish gray sandstone, thick bedded, and display mudstone intercalation. It is rarely fossiliferous reported, the fauna includes orbitoides mostly, but overall, it is poorly fossiliferous. In Zindapir area, it has upper unconformable contact with Khadro Formation and attains thickness up to 446 m, while being 469m thick in principle section. The sandy beds are devoid of any fossil content, but an assemblage of benthonic foraminifera has been recorded within the shales and is considered to be of Cretaceous age (Kadri. 1995).

In the Central Indus Basin, the Pab Formation is restricted to the southwestern and central areas; in the north and east, sediments of Upper Cretaceous age are probably absent. The sediments consist of thickly bedded, coarse-grained sandstones, with thin layers of calcareous shale in the lower unit. The Deposition of the Formation probably occurred in a marine shelf location, where the general lowering of sea level provided a significant source of sediment.

2.2.2.8 Fort Munro Formation

The Limestone is fossiliferous and contains the remains of reef-building organisms such as hermatypic corals, ammonites, and echinoids, as well as abundant bioclastic debris, probably derived from

bivalves. It has dark grey to black, medium to thick bedded limestone with alternating thinly bedded gray marly shale. The Fort Munro Formation is argillaceous in the lower part and sandy in the upper part. The faunal assemblage of the Formation includes foraminifera, especially orbitolites.

In Zindapir area, it has upper transitional contact with Pab Formation and attains thickness up to 139 m and it is about 100 m thick in the principal at Fort Munro Anticline, near the Dera Ghazi Khan Road. It is upper Campanian to upper Maastrichtian age based on the benthonic foraminiferal index species (Iqbal and Shah, 1980), and displays a shallow marine shelf environment.

2.2.2.9 Mughal Kot Formation

It is calcareous mudstone of gray color, with limestone and shale intercalations. The sandy upper unit displays a rare fossiliferous nature in places. The biota assemblage of the Mughal Kot Formation includes shallow benthic foraminifera's orbitoides media, omphalocyclus macroporus, and siderolites calcitrapoides, while the planktonic foraminiferal microfauna comprising Globotruncana spp., Globigerina spp., Guembelina spp., and associated forms has also been recorded, but the assemblage is usually impoverished (Kadri, 1995). In Zindapir area, the base of the Mughal Kot Formation is buried, while its upper conformable contact is with the Fort Munro Formation. It is about 172 m in Zindapir area, while it is about 1170 m thick in its principal section at Mughal Kot (Kadri, 1998)

CHAPTER #3

Methodology

3.1 Introduction

The Habib Rahi Formation of the Zindapir Anticline is selected for reconnaissance and samples were collected for geotechnical investigation. For the purpose of determining the geological suitability, workability, and economic potential, all outcrop characteristics—including the lithology, bedding pattern, colour, texture, contacts, etc., were studied. Samples were then transported for further investigation, like petrography and crushing for engineering testing.

3.2 Fieldwork

The three days of fieldwork were conducted in Zindapir Anticline, Dera Ghazi Khan, Pakistan. In the study area, the Habib Rahi Formation was the main focus for geotechnical investigation studies on an outcrop scale as well as in hand specimens. The Habib Rahi Formation is thin to medium bedded limestone with chert beds and shale intercalation. The color of limestone on a fresh surface is pale yellow. For the petrographic examination, four samples from the Habib Rahi Formation outcrop were used, and for the geotechnical research, samples were brought to the SABHAN Geotechnical Laboratory to be examined for their physical and mechanical characteristics.

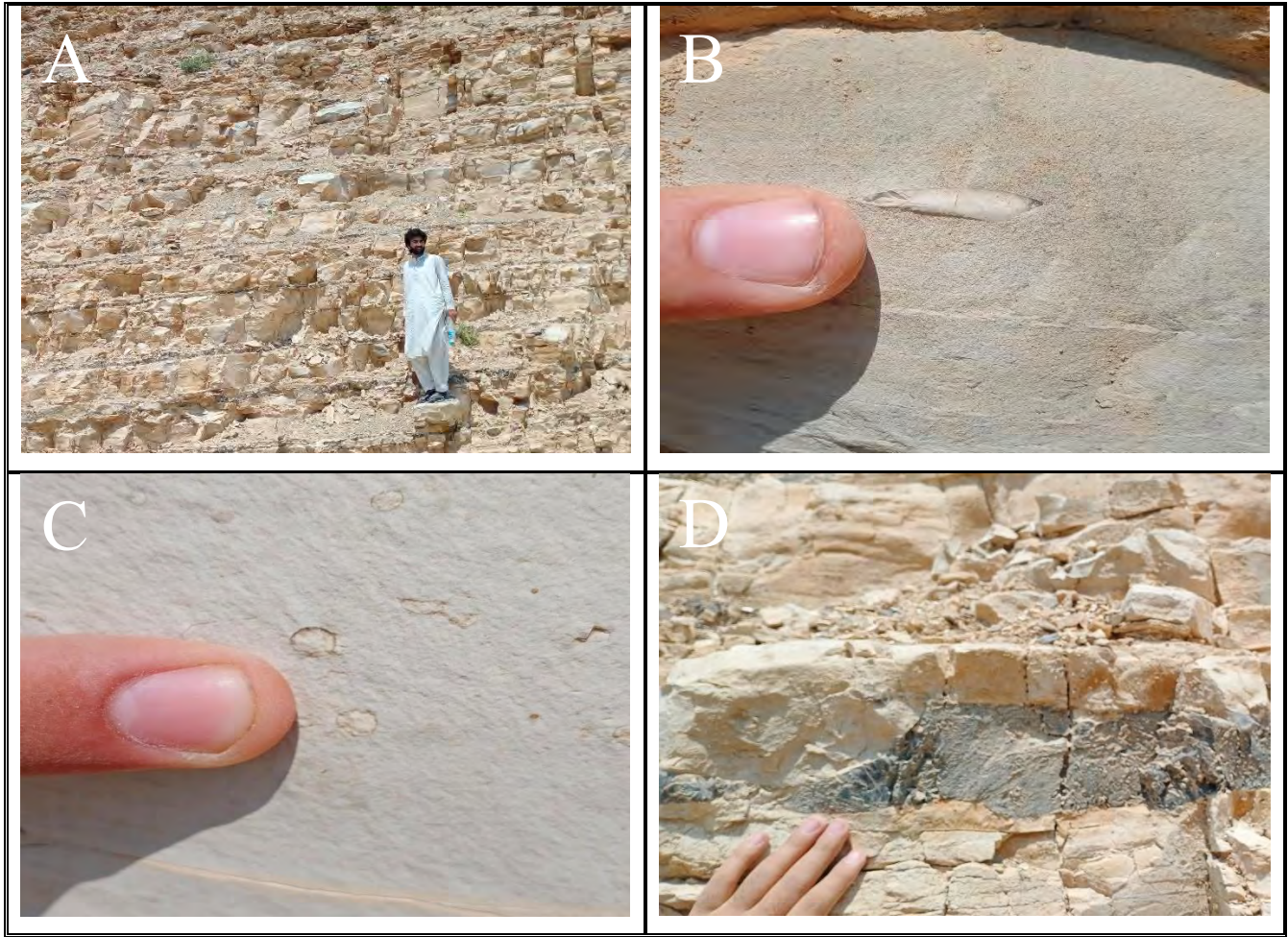


Fig 3.1 Field photographs of Habib Rahi Formation (A) Road cut section (B, C) benthic foraminifera (D) Chert Bed.

3.3 Laboratory work

3.3.1 Petrographic analysis

Various geotechnical tests were performed on the samples using approved techniques created in advance by the ASTM, AASHTO, and BS standards. In order to select reasonable quality and performance-bound aggregate for use in the construction projects, physical, mechanical, and chemical testing was carried out in accordance with the required specifications on all typical samples. Characterizing the aggregate is crucial. To make sure the necessary requirements were achieved, testing were performed using physical, mechanical, and chemical methods. The alkali aggregate reaction potential (ASR) of these aggregates was also evaluated petrographically. To decrease the possibility of errors and assure accurate results, each sample was examined four times. For the following tests, the represented samples were cleaned and dried in the lab.

The reactive components in aggregates are routinely identified via petrographic studies [ASTM C125-03, 2003]. Determining the mineral composition and texture of the rock's aggregate is the primary objective of current petrographic research.

3.3.2 Geochemical test

3.3.2.1 XRF

X-ray fluorescence is a commonly adopted method in various experimental studies that can analyze major and trace elements and their corresponding major and trace oxides quickly and precisely. Rocks and soils are routinely analyzed using this technique (Recenko, 2002).

3.3.2.2 ASR ASTM C-1260

This test method offers way to identify an aggregate's ability to undergo an alkali silic reaction that could lead to potentially damaging internal expansion. It is especially useful for aggregates that respond slowly or cause expansion later in the reaction of alkalis and silica. The usage of aggregates in conjunction with cementitious materials, as well as test conditions resembling those that concrete will encounter in practical uses, are not evaluated, however (Monnin, 2006). The specimens are subjected to a NaOH solution, so the alkali content of the cement has little impact on expansions. It is recommended that additional data be collected to confirm that excessive expansions are actually caused by the alkali-silica reaction when they are noticed. The use of mitigating measures, such as low-alkali Portland cement, mineral admixtures, or ground granulated blast-furnace slag, should be taken into account when tests using this test method and additional information show that a specific aggregate should be regarded as potentially deleteriously reactive



Figure 3.2 ASR test in progress at PCSIR Peshawar.

3.3.3 Physical test

- **Specific gravity and water absorption rate according to AASHTO T-85/ASTM C 127.**

This test method assesses the density of the predominantly solid portion of a multitude of aggregate particles, yielding an averaged outcome that serves as a representation of the sample. The density of aggregate particles, as determined by this test method, differs from the bulk density of aggregates calculated by Test Method C 29/C 29M, as the latter accounts for the volume of voids present between aggregate particles.

For 24 ± 4 hours, a sample of aggregate is submerged in water to practically fill the pores. After being taken out of the liquid, the particles' surface is dried and their mass is calculated. Following that, the sample's volume is calculated using the movement of water method (ASTM C 127). The sample is then oven-dried, and the mass is calculated. It is feasible to determine density, relative density (specific gravity), and absorption using the mass values consequently determined and the calculations in this test technique.

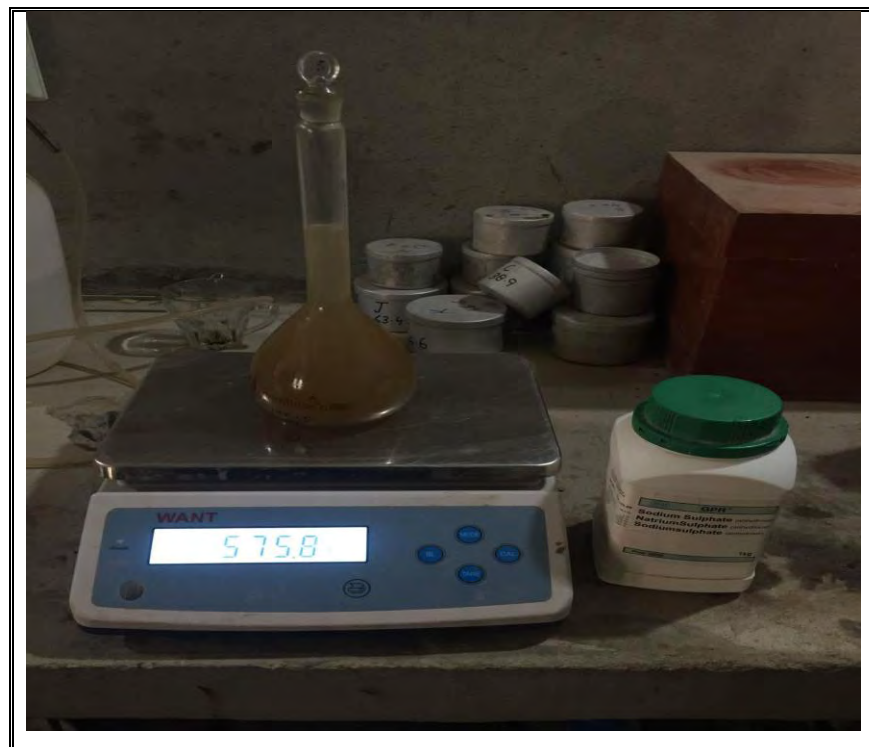


Fig 3.3 Specific Gravity test in progress at SABHAN Geotechnical Laboratory.

- **Sieve analysis for coarse aggregate AASHTO T-27**

In a set of nested sieves, the top sieve has the largest screen openings, and the size of the openings decreases with each sieve down to the bottom sieve, which has the smallest opening size screen for the type of material specified. A known weight of material, the amount being determined by the largest size of aggregate, was placed upon the top of the set of sieves and mechanically shaken for a period of time. The material retained on each sieve is weighed after the material has been shook through the nested sieves. In order to use the cumulative method, each sieve must be weighed before being added to a pan that has already been weighed (known as the tare weight), which was previously filled with the contents of the previous sieve.



Fig 3.4 Sieve Analysis in progress at SABHAN Geotechnical Laboratory.

- **Particles shape (Flakiness and elongation) according to ASTM D-4791-99**

The amount of flat particles, elongated particles, or flat and elongated particles in coarse aggregates can be determined using this test procedure. To calculate the ratios of width to thickness, length to width, or length to thickness, specific aggregate particles are measured. This test method offers a way to determine the relative form characteristics of coarse aggregates or evaluate compliance with standards that restrict such particles.

A particle is considered elongated if its length is greater than 1.8 times the average sieve size of the size fraction to which it belongs. If the thickness of the particle is less than 0.6 times the mean sieve size of the size fraction, it is also considered to be flaky. Elongated and flaky particles make concrete mix less workable because they have a big surface area compared to a limited volume. Because the flaky particles are frequently orientated in a single plane, water and cavities might accumulate there and reduce the durability of the concrete. It is not desirable to have flaky or elongated particles that comprise more than 10% to 15% of the weight of the coarse aggregate. Aggregate sizes ranging from 63 mm to 6.3 are used in the test.

3.3.4 Durability test

- **Loss Angeles test according to ASTM C131-06 (2006)**

This test method covers a procedure for testing sizes of coarse aggregate smaller than 37.5 mm (1 1/2 in.) for resistance to degradation using the Los Angeles testing machine.

A rotating steel drum containing a predetermined number of steel spheres, the number based on the grading of the test sample, is used to measure the degradation of mineral aggregates of standard grading as a result of a combination of actions such as abrasion or attrition, impact, and grinding. The sample and the steel spheres are pulled up by a shelf plate as the drum turns and are carried around until they are deposited to the opposite side of the drum, where they impact and crush. When the shelf plate takes up the sample and the steel spheres, it grinds the contents of the drum roll within it in an abrading and grinding motion, and the cycle is then repeated. The contents are evacuated from the container after the required number of revolutions. The contents of the drum are removed after the required number of revolutions, and the aggregate portion is sieved to calculate the deterioration as a percent loss.



Fig 3.5 Loss Angeles abrasion test in progress at SABHAN Geotechnical Laboratory.

- **Soundness test according to AASHTO-T-104-99/ASTM C88.**

This test method is applicable for evaluating the soundness of aggregates when subjected to weathering action in concrete or other applications. This is performed by repeatedly immersing the aggregates in saturated sodium- or magnesium-sulfate solutions, followed by partially dehydrating the precipitated salt within the permeable pore spaces through oven drying. The internal expansive force, resulting from the salt's rehydration upon re-immersion, resembles the expansion of water when it freezes. This test method provides valuable information for assessing the soundness of aggregates in cases where sufficient data is not accessible from the service records of materials exposed to real-world weathering conditions.

This test method specifies a mechanism for estimating the soundness of aggregates for use in concrete and other operations. The obtained values can be compared with specifications, for example consider specification C-33, which is intended to convey the acceptability of suggested use aggregates. While the test is typically tougher when magnesium sulfate is used, the maximum permitted percent loss is typically higher than it is when sodium sulfate is used.



Fig 3.6 Soundness test in progress at SABHAN Geotechnical Laboratory.

3.3.5 Mechanical test

- **Aggregate Impact Value BS-812-112. (1990)**

This section of BS 812 discusses techniques for calculating the aggregate impact value (AIV), which is an approximate measure of an aggregate's resistance to unexpected shock or impact. A test specimen is compacted into an open steel cup in a standardized manner. Following that, the specimen undergoes a series of standard impacts from a dropped weight. This action breaks the aggregate to various degrees depending on the material's impact resistance. The aggregate impact value (AIV) is calculated using a sieving procedure on the impacted material to determine this degree.



Fig 3.7 Aggregate Impact Value machine at SABHAN Geotechnical Laboratory.

- **Aggregate crushing value BS-812-110. (1990)**

This section of BS 812 defines a procedure for calculating the aggregate crushing value (ACV), which provides a comparative assessment of an aggregate's resistance to crushing under a compressive stress that is delivered progressively. A test sample is uniformly compressed into a steel cylinder with a freely rotating plunger. After that, a typical loading regime is administered through the plunger to the specimen. Depending on the material's resistance to crushing, this operation will crush the aggregate to a different extent. This degree is used as a gauge for the aggregate crushing value (ACV) and is determined by a sieving test on the crushed specimen.

Unit Weight ASTM C29/C 29M AASHTO No.: T19/T19M

This test method involves the calculation of voids among particles within fine, coarse, or mixed aggregates, relying on the determination of the bulk density (referred to as "unit weight") of the aggregate in either a compacted or loose state. This test method is appropriate for aggregates with a nominal maximum size of 5 in. [125 mm].

The bulk density values required for use in many methods of choosing proportions for concrete mixtures are frequently determined using this test method. Calculating the mass/volume relationships for

conversions in purchase agreements can also be done using the bulk density. The degree of compaction of aggregates in a hauling unit or stockpile and that attained in this test method are not known to be correlated, though. Additionally, even though this test method determines bulk density on a dry basis, aggregates in transporting units and stockpiles generally include absorbed as well as surface moisture (the latter of which has an impact on bulking). This test method's bulk density, which is used as the foundation for the calculation of the percentage of voids between aggregate particles, is included.

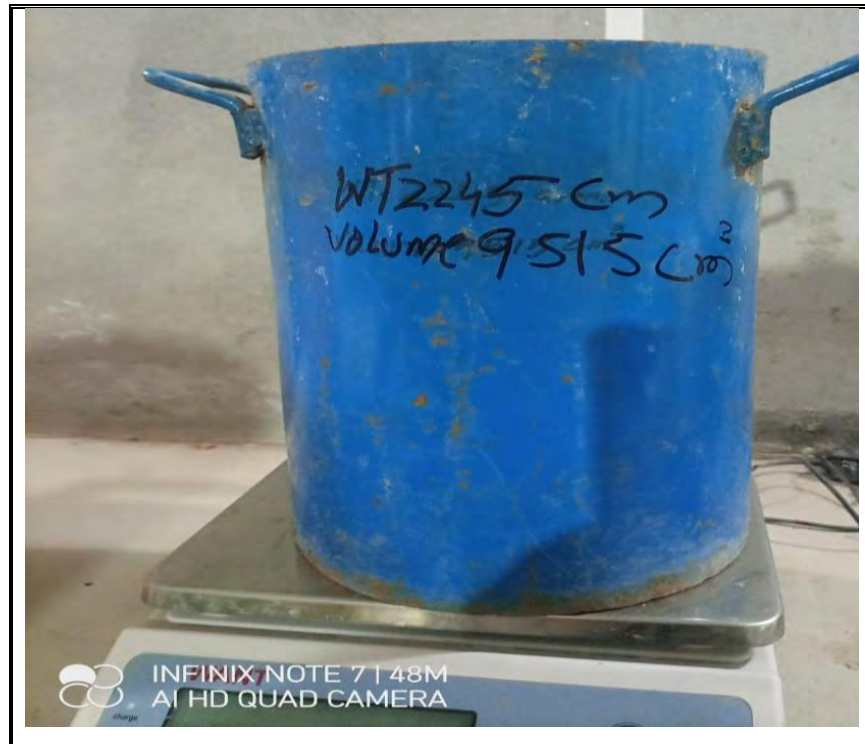


Fig 3.8 Unite weight instruments.at SABHAN Geotechnical Laboratory.

3.3.6 Bituminous test

- **Stripping and Coating test of aggregate AASHTO-T-182-84. (2002)**

The coating and static immersion processes for assessing the ability to retain of a bituminous coating on an aggregate surface when there is water are described in this approach. It can be used with cutback, and semi-solid tars and asphalts. At a specific temperature suitable to the bitumen grade being utilized, bitumen is applied to the chosen and prepared aggregate. The bitumen-coated aggregates is heated to 60 C (145 F) during a curing phase for cut back asphalt and tar. When using emulsified asphalt, the aggregate is covered with bitumen and heated to 135 C (275 F) during the curing process. The coated aggregate is submerged in distilled water for 16 to 18 hours after coating, or after curing, in the case of semi-solid asphalt and tar, or in the case of cutback asphalt, emulsified asphalt, and tar. When the bitumen-

aggregate mixture has finished soaking and is submerged, the amount of aggregate on the bituminous coating that has been retained can be visually considered to be above or below 90%.

CHAPTER #4

Petrography and Geochemistry

4.1 Introduction

Petrography is one of the most basic and essential studies of rocks and focuses on the detailed description of the rock's mineral content. To better understand the potential influence of these diagenetic and depositional fabrics on the engineering properties of the studied rocks. To identify the various depositional and diagenetic fabrics, detailed petrography was conducted in accordance with ASTM C295 (2012). Petrographic features of rocks have a significant impact on their mechanical properties. By examining its texture, mineralogical composition, and weathering, petrographic investigation of rock provides important insights about its mechanical behavior under stress (Irfan 1996). The Habib Rahi Limestone underwent a petrographic examination in accordance with ASTM C 295. ASR potential, which has an impact on the durability of hardened concrete (López-Buenda et al. 2006), is explained by the study carried out under petrographic microscopic conditions (French, 1991). Chert beds are interbedded in Habib Rahi limestone, which forms through diagenesis that describes the process through which sedimentary rocks undergo physical and chemical changes after early deposition (Knauth, L. P. (1979). Chert is primarily composed of microcrystalline quartz, and it forms when silica-rich fluids percolate through limestone beds, depositing silica in the pore spaces and fractures of the rock. Over time, this silica accumulates and solidifies, forming chert beds within the limestone. To identify harmful components in the aggregate, it is essential to understand the petrography of the Habib Rahi Formation. Additionally, it will also assist in revealing the diagenetic changes that influence the engineering qualities of rocks.

4.2 Sample Collection

Five representative fresh rock samples were collected during the fieldwork on the basis of mineralogy and texture relationships. A sample location map is provided (Fig 1.1). Out of these five rock samples, one sample is from chert beds for petrographic analysis, and the remaining samples were collected for physico-mechanical investigation, and chips were cut and finished into thin sections for detailed Petrographic studies (Table 4.1).

4.3 Thin Section Preparation

For this research, rock samples were cut into chips and 0.03 mm thick thin sections were prepared using the technique in rock cutting lab at Earth Science Department, Quaid-I-Azam University Islamabad. The prepared thin sections were finally studied in Petrography Lab of Earth Science Department, Quaid-I-Azam University Islamabad, on Leica DM750P Polarizing Microscope.

4.4 Petrographic details

The limestone of the Habib Rahi formation of Zindapir anticline in hand specimen, is light gray on fresh surface and yellowish to grayish on weathered surface (Fig 3.1). In thin sections, the Habib Rahi limestone is dominantly composed of calcite, microfossils. As illustrated in Fig. 4.8, one sample of the investigated rocks is medium-grained and primarily composed up of fossilized shells, while the other samples are fine to medium-grained with granular mosaic texture and microfossils. (Table 4.1) displays the model mineralogy of the examined rock sample. Calcite is fine-grained and ranges in percentage from (58–88%); nevertheless, some patches, as seen in (Fig 4.7 and 4.8), are medium-grained. HR-1 sample is dominantly composed of calcite, which is a fine grained ground mass, broken shell fragments and pyrite grains are embedded in the matrix (Fig 4.1, 4.2). However, HR-2 and HR-3 are also composed of fine grained ground mass micrite and bioclast embedded in a fine grain matrix (Fig 4.3-4.6). Calcite filled fractures are observed in HR-2 as shown in (Fig 4.4). Moreover, HR-4 are dominantly composed of micrite and medium grained bioclast. Micro-fracture were also as observed in the shells of the microfossils. The micrite, which is composed of fine-grained calcite, contributes both a ground mass and a cement for the fossils. HR-5 thin section were prepared and examined for chert beds in limestone, which are dominantly composed of silica grains that are cemented in a fine grained matrix as shown in (Fig 4.9, 4.10). It is said that Habib Rahi formation limestone of Zindapir anticline has no deleterious mineral to produce alkali silica reaction (ASR) in concrete, which is further explained in detail. The studied limestones can be classified as “Mudstone-Wackstone” according to Dunham’s (1962) classification scheme.

Table 4.1 Model composition of Habib Rahi Formation at Zindapir anticline.

Dunham Classification	Sample No.	Micrite %	Sparite %	Total calcite %	Bioclast %	Authigenic Minerals %
Mudstone	HR-1	78%	10%	88%	8%	4%
Mudstone	HR-2	66%	10%	76%	21%	3%
Mudstone	HR-3	60%	13%	73%	23%	4%
Wackstone	HR-4	47%	11%	58%	38%	4%
<i>Chert bed</i>	HR-5	19%	-	19%	6%	75%

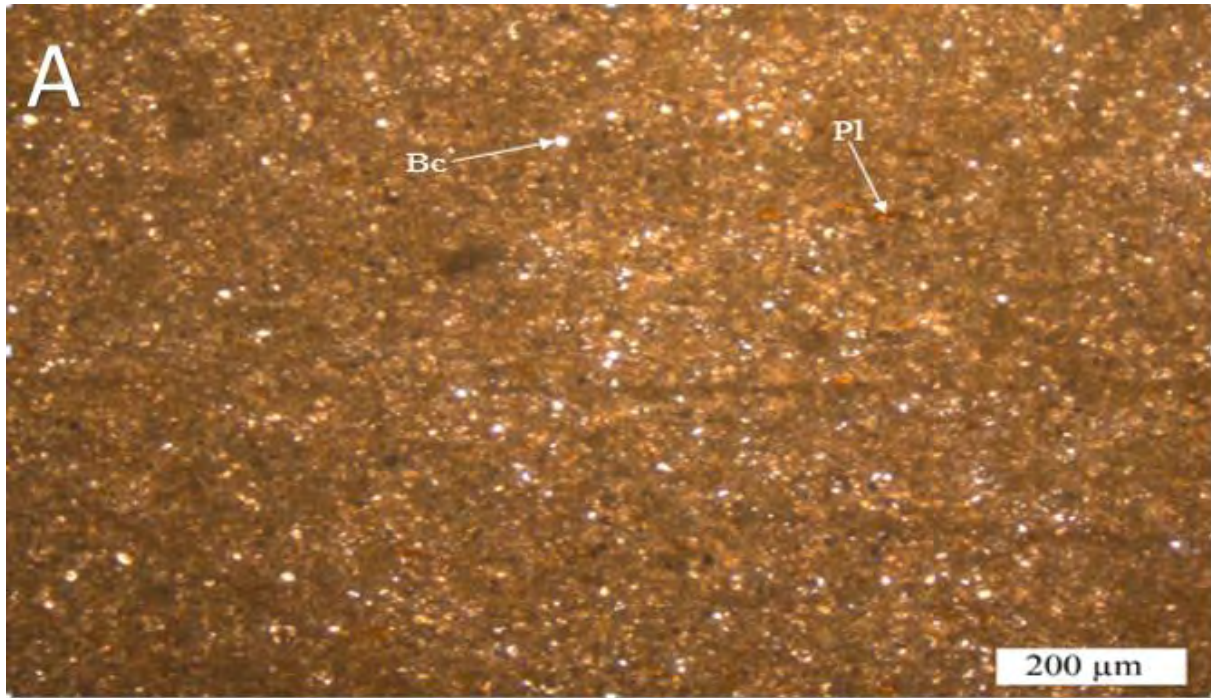


Fig 4.1 Photomicrograph of Habib Rahi Limestone (HR-1) showing Bioclast (Bc), Pyrite leaching (Pl).

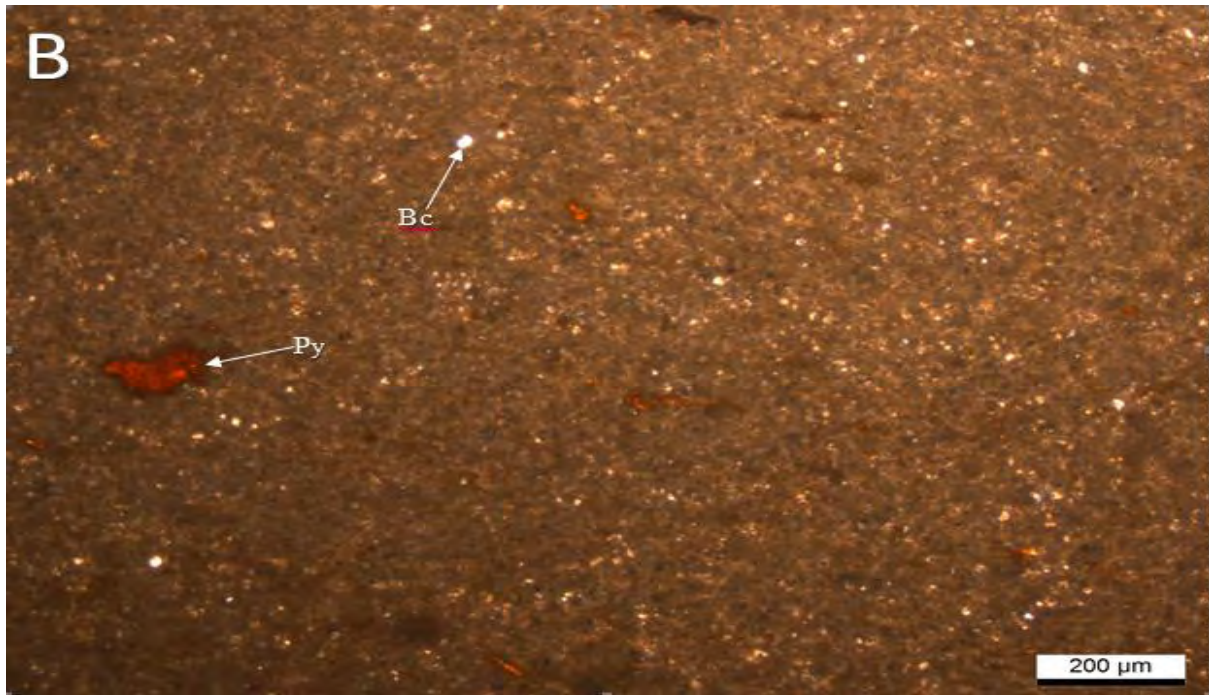


Fig 4.2 Photomicrograph of Habib Rahi Limestone (HR-1) showing Bioclast (Bc), and Pyrite leaching (Pl).

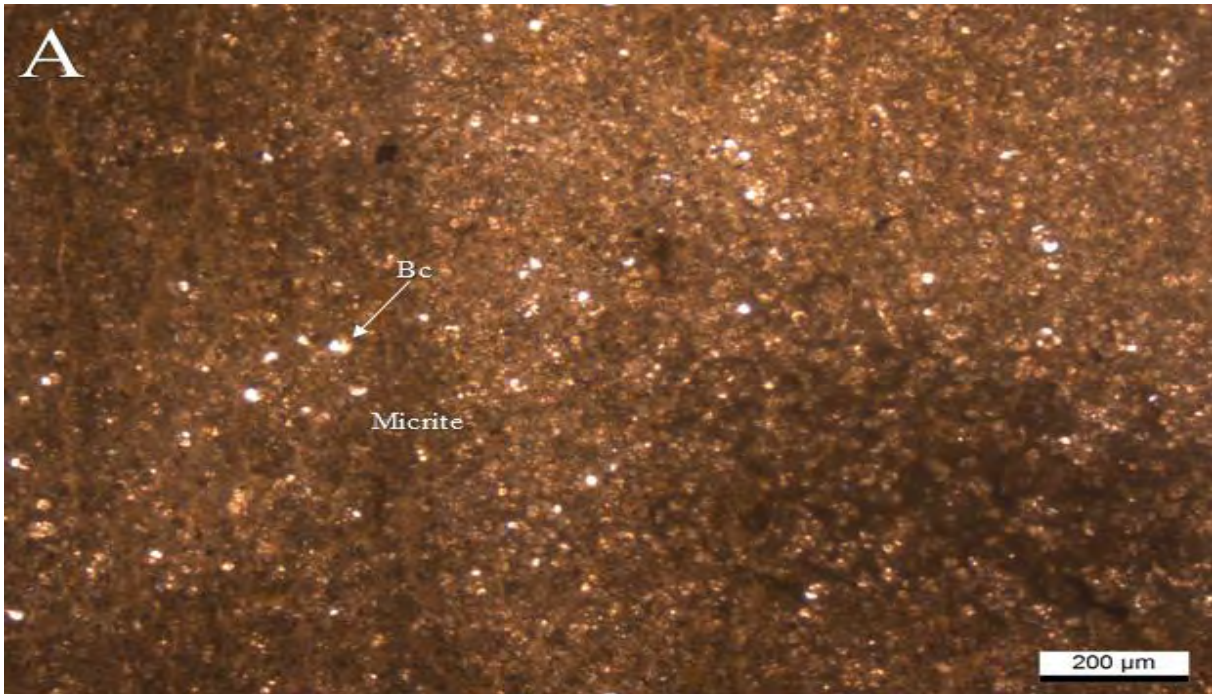


Fig 4.3 Photomicrograph of Habib Rahi Limestone (HR-2) showing Micrite, and Bioclast (Bc).



Fig 4.4 Photomicrograph of Habib Rahi Limestone (HR-2) showing Fracture (Fr), and Pyrite leaching (Pl).

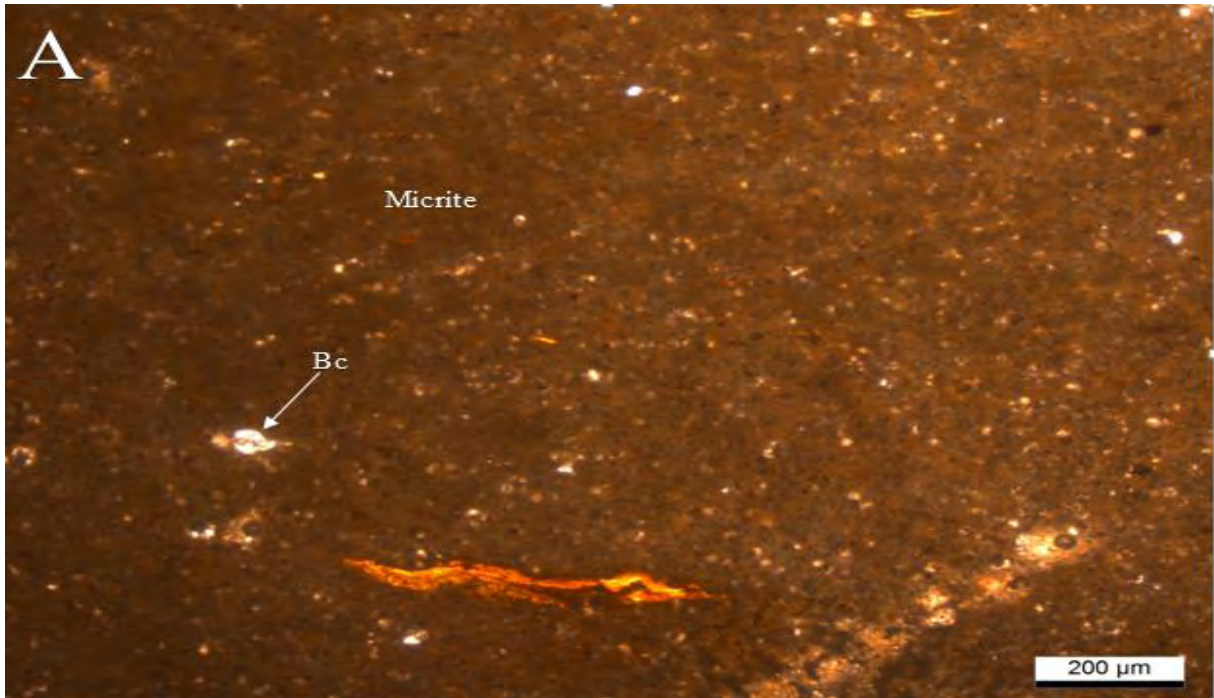


Fig 4.5 Photomicrograph of Habib Rahi Limestone (HR-3) showing Bioclast (Bc), Micrite.

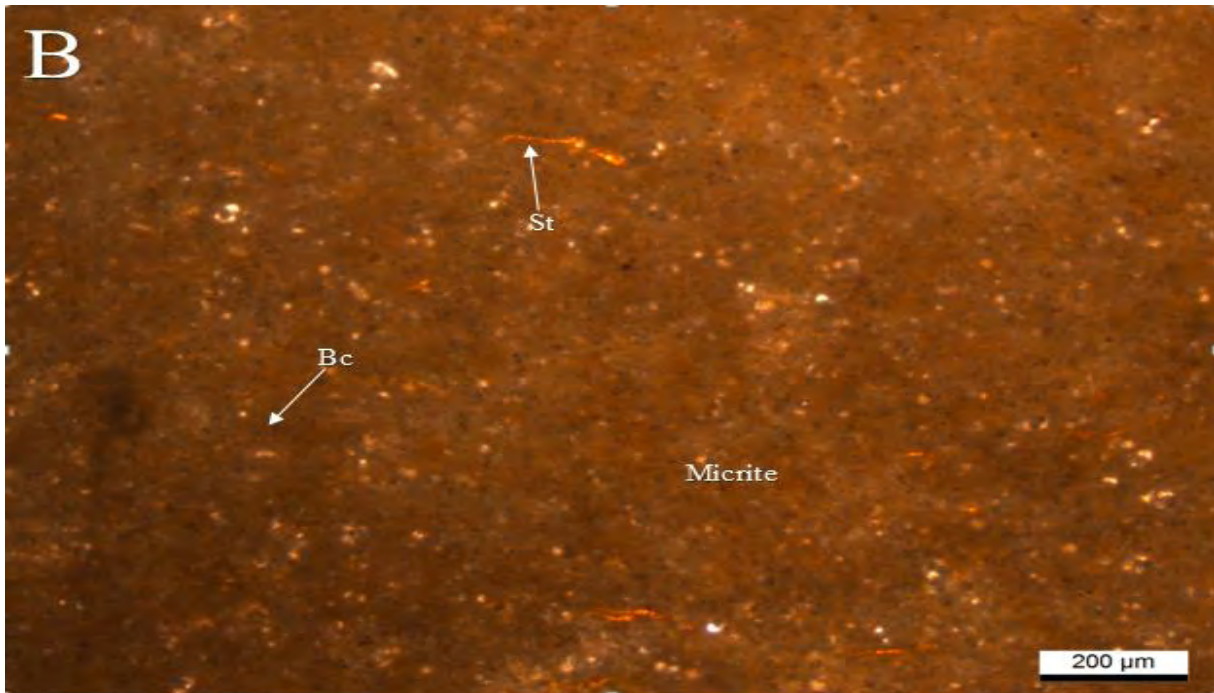


Fig 4.6 Photomicrograph of Habib Rahi Limestone (HR-3) showing Bioclast (Bc), Micrite, and Stylolite (St).

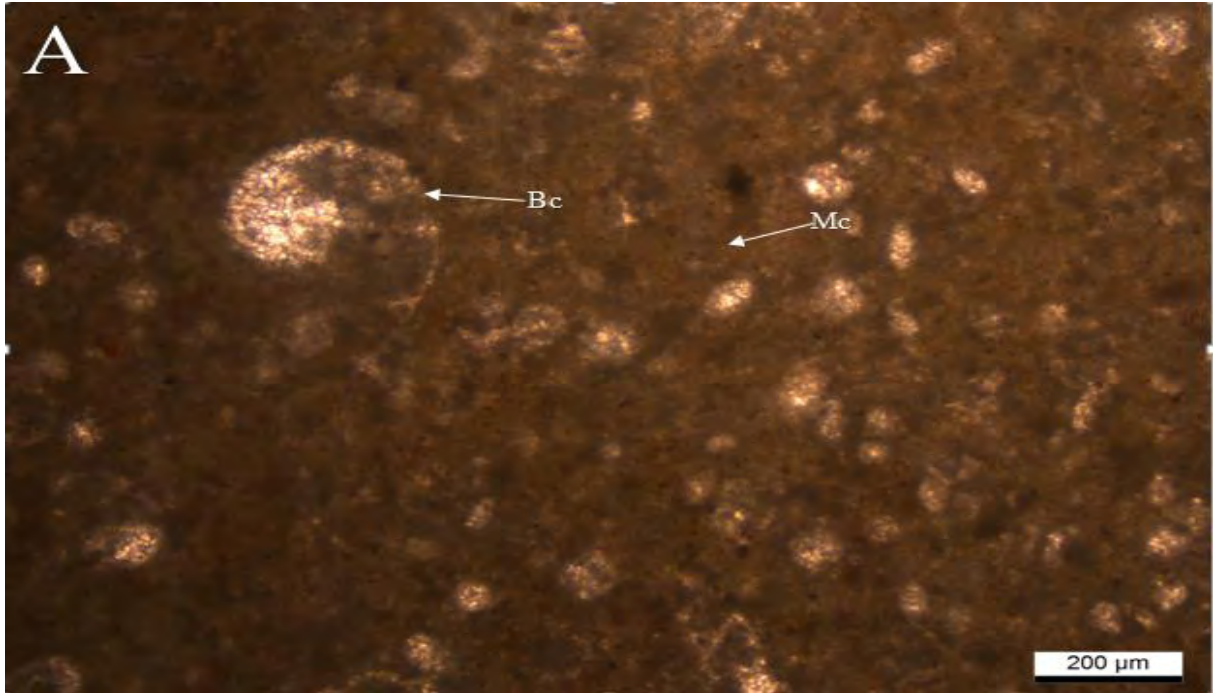


Fig 4.7 Photomicrograph of Habib Rahi Limestone (HR-4) showing Micrite (Mc), and Bioclast (Bc).

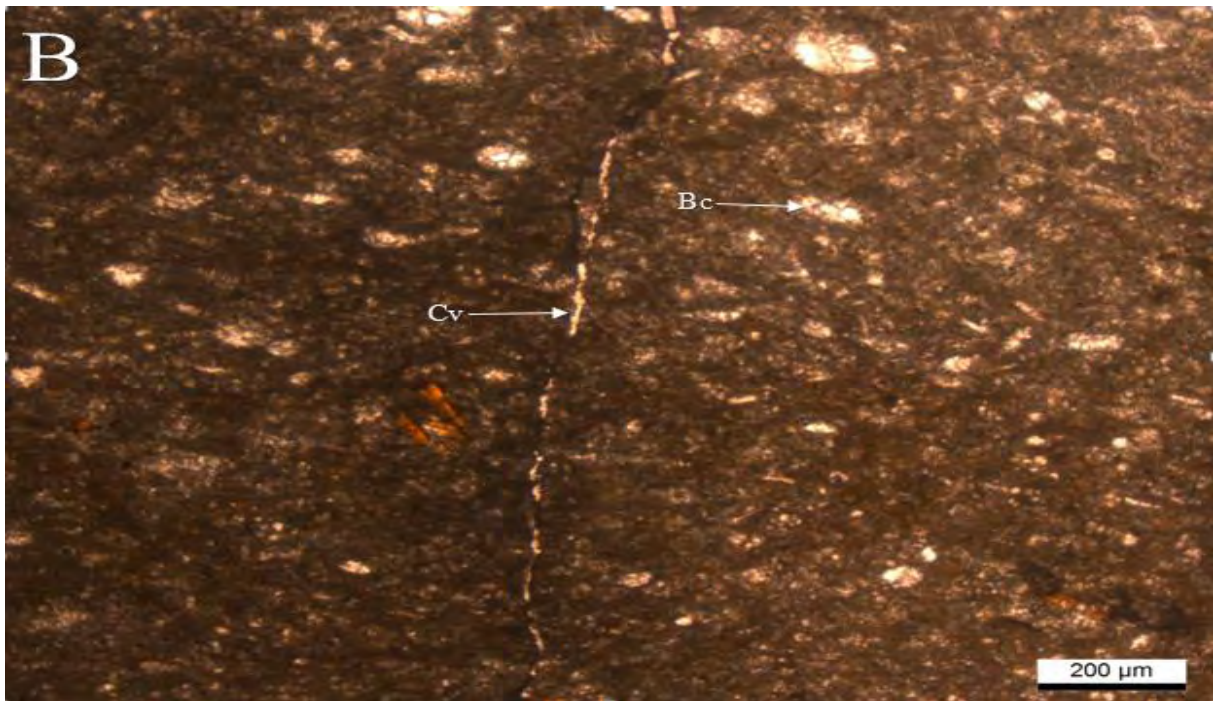


Fig 4.8 Photomicrograph of Habib Rahi Limestone (HR-4) showing Calcite vein (Cv), and Bioclast (Bc).

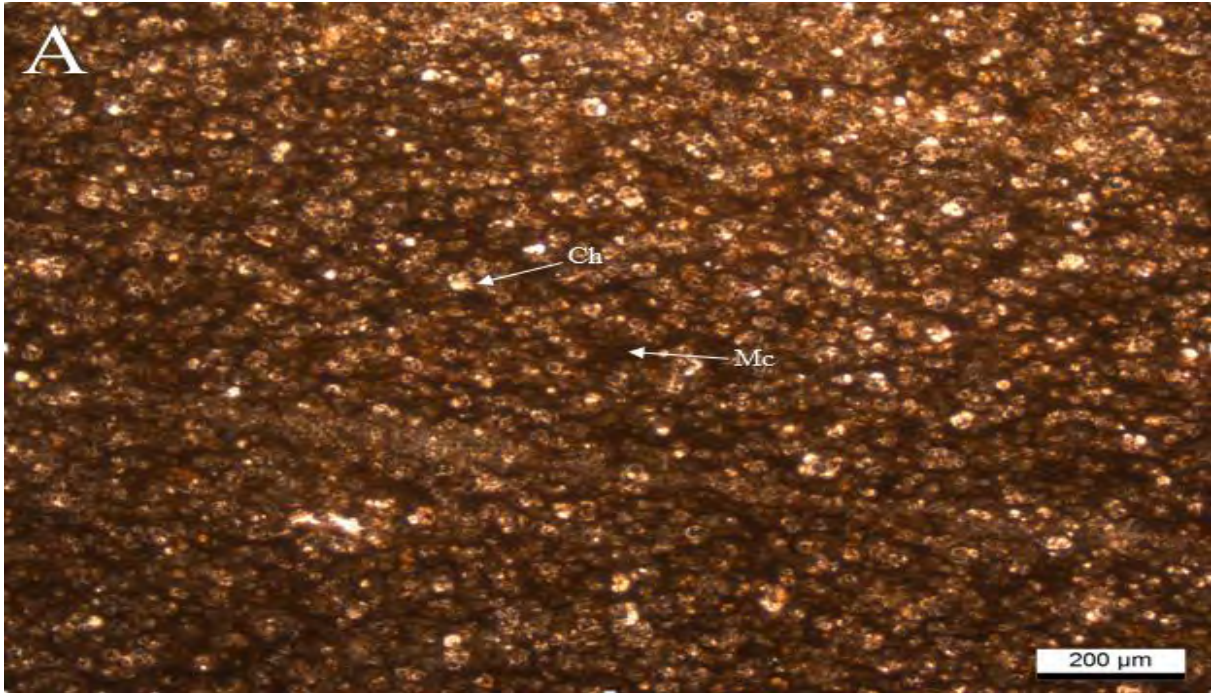


Fig 4.9 Photomicrograph of Habib Rahi Limestone (HR-5) showing Chert grains (Ch), and Micrite (Mc).

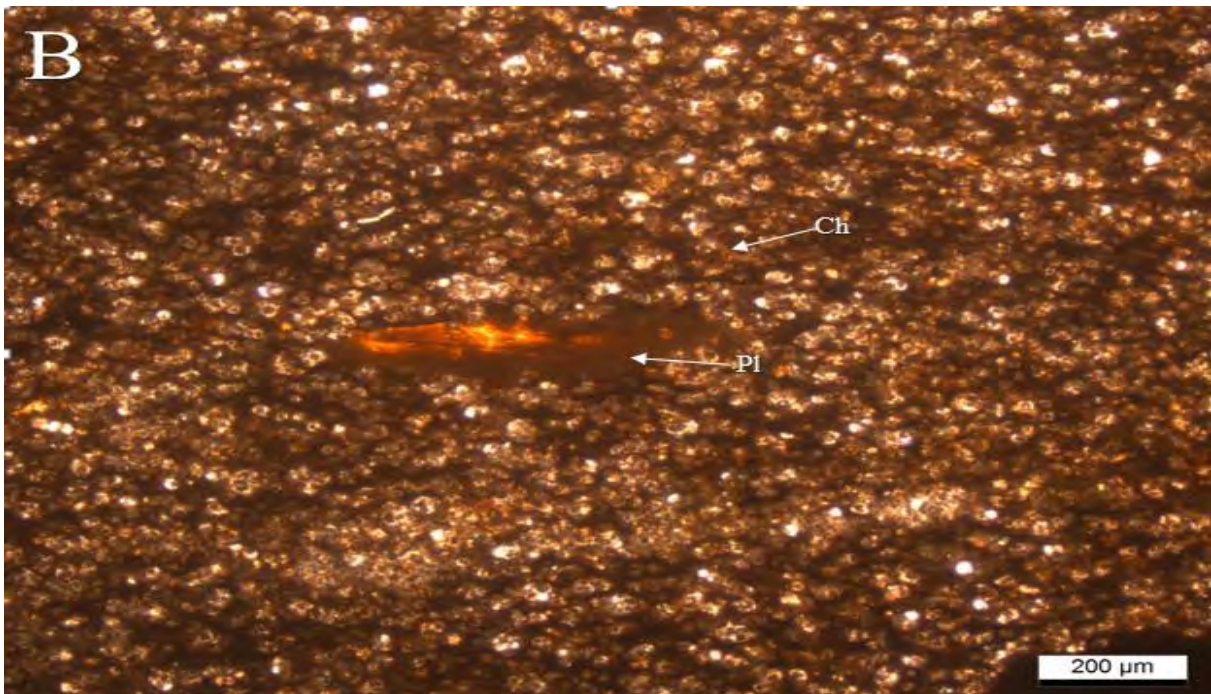


Fig 4.10 Photomicrograph of Habib Rahi Limestone (HR-5) showing Chert grains (Ch), and Pyrite leaching (Pl).

4.5 Geochemical test

4.5.1 Introduction

The primary and most crucial tool for examining the petrology of any region is geochemical analysis. It contributes to the classification of rocks into different groups and subgroups and offers information on the different types of magma, their differentiation, and their origins based on tectonic settings. In addition, the geochemical information supports and confirms the petrographic research. Four solid rock samples were chosen for geochemistry for this purpose based on thin section studies and lithological variations.

PXRF has been frequently used as a research and exploration tool to determine elemental variability among siliciclastic mudrocks, during the past decade (Dahl et al., 2013) (Nance and Rowe, 2015) (Turner et al., 2016). Consequently, mudrock-based quantification procedures (e.g., Rowe et al., 2012) are frequently used for converting PXRF photon count data to elemental concentrations in a variety of sedimentary lithologies. In spite of the general understanding that compositional and matrix effects can have a negative effect on data quality (e.g., Brand and Brand, 2014; Craigie, 2018). In the study by (Quye-Sawyer et al., 2015), Based on the manufacturer's calibration (mudrock calibration), PXRF photon counts from limestones were transformed to elemental concentrations. The authors presented a series of correction factors that could be used with the quantification approach given by the instrument maker to account for the lithological variations between siliciclastic mudrocks and limestones. The author's reasoned that such an approach might provide more accurate elemental concentrations. A few details were provided, however, about the measurement of raw PXRF photon counts or the conversion of raw data to elemental concentrations. As far, there is still much work to be accomplished in the field of analytical geochemistry.

4.5.2 Sample Preparation

A total four fresh bulk rock samples were selected for geochemical analysis (Table 4.1). These rock samples were collected from the Habib Rahi Formation. The analysis was done using portable X-ray Fluorescence Spectrometry (PXRF) for major oxides. Whole rock samples were washed with distilled water and a scrub brush before examination in an effort to remove surface impurities such as leftover drilling mud. Surfaces were then wiped clean with a towel and blown dry with compressed air. To obtain powder samples, pre-cleaned whole rock samples were crushed and standardized by hand using an agate mortar

and pestle. Pressed powder pellets were prepared from a portion of the ready powders. These powders were then pressed mechanically to get consolidated powder pellets.

Table 4.2 Geochemical analysis of various samples of Habib Rahi limestone.

Sample No.	CaO	SiO ₂	Fe ₂ O ₃	Al ₂ O ₃	K ₂ O	TiO ₂
HR-1	48.62%	5.97%	1.09%	1.28%	0.20%	0.14%
HR-2	47.25%	5.54%	1.26%	1.35%	0.29%	0.16%
HR-3	51.00%	5.69%	1.17%	1.16%	0.21%	0.09%
HR-4	48.32%	5.38%	1.34%	1.32%	0.17%	0.14%



Fig 4.11 Graphical comparison of CaO in the collected rock samples of Habib Rahi Formation.

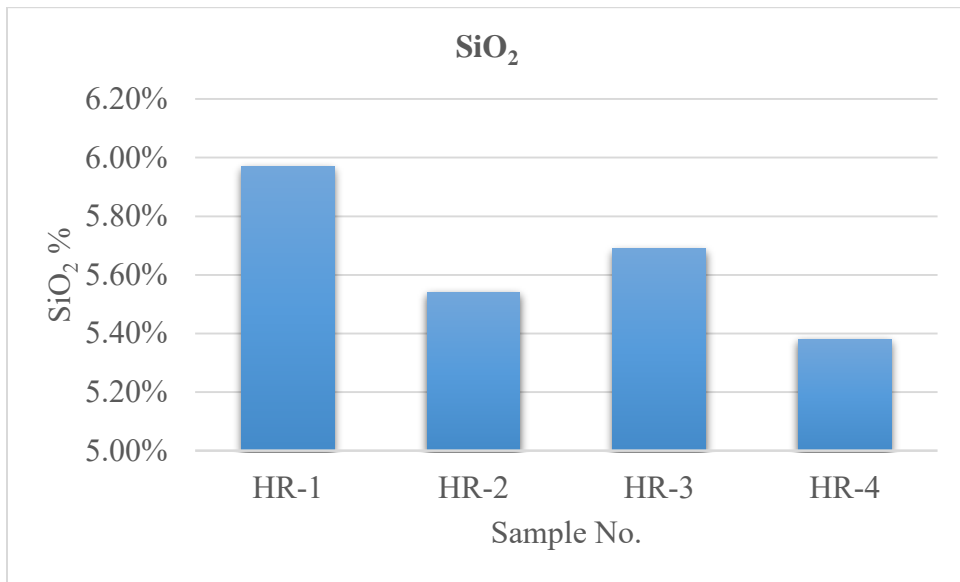


Fig 4.12 Graphical comparison of SiO₂ in the collected rock samples of Habib Rahi Formation.

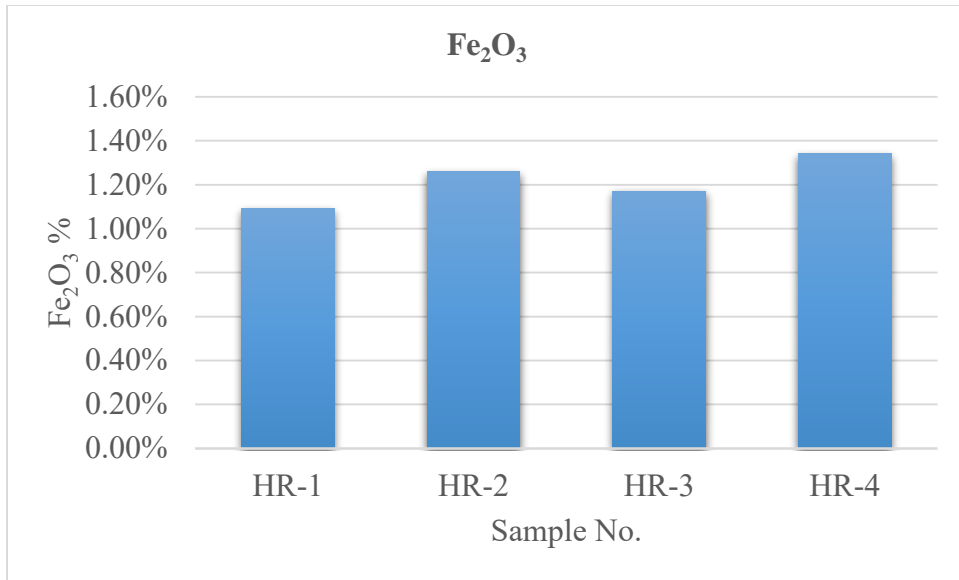


Fig 4.13 Graphical comparison of Fe₂O₃ in the collected rock samples of Habib Rahi Formation.

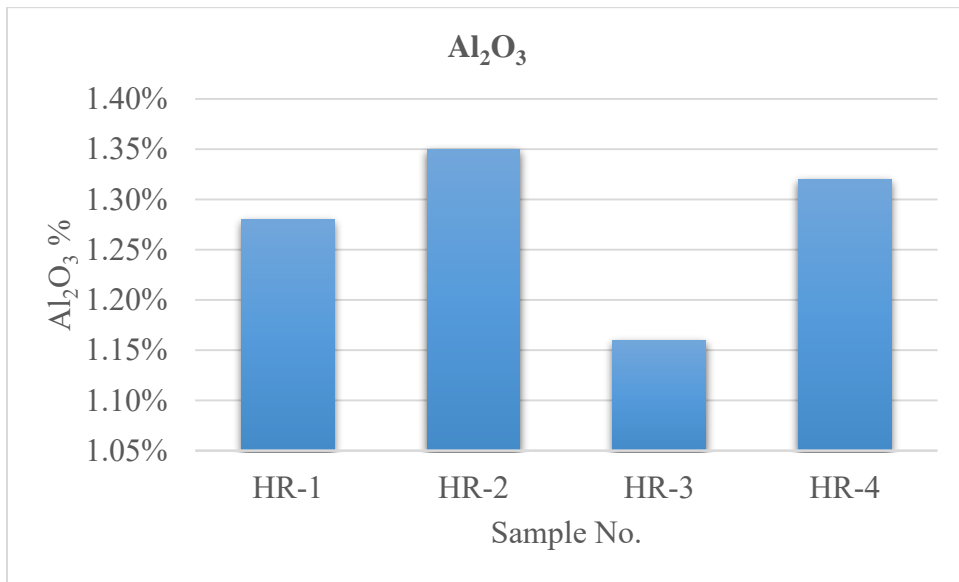


Fig 4.14 Graphical comparison of Al₂O₃ in the collected rock samples of Habib Rahi Formation.

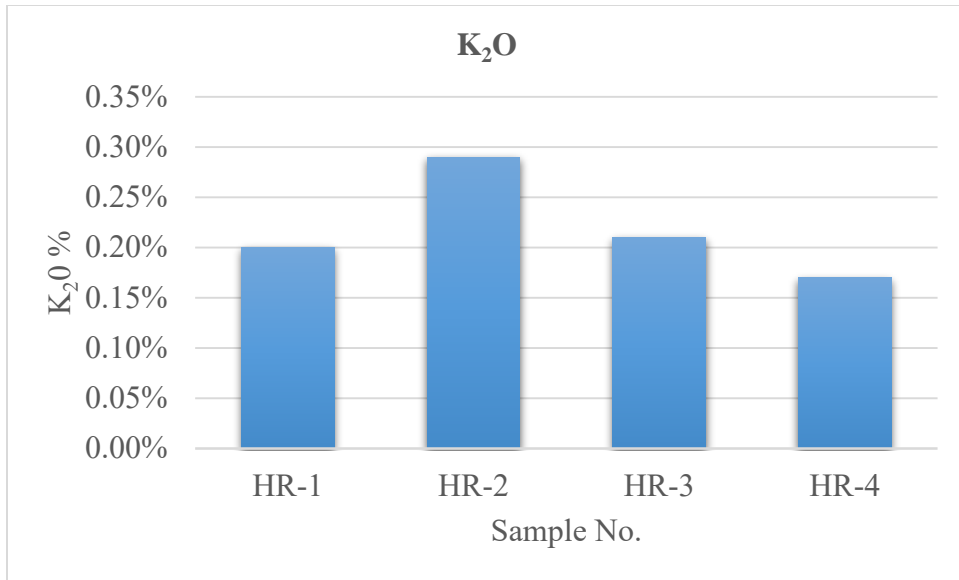


Fig 4.15 Graphical comparison of K₂O in the collected rock samples of Habib Rahi Formation.

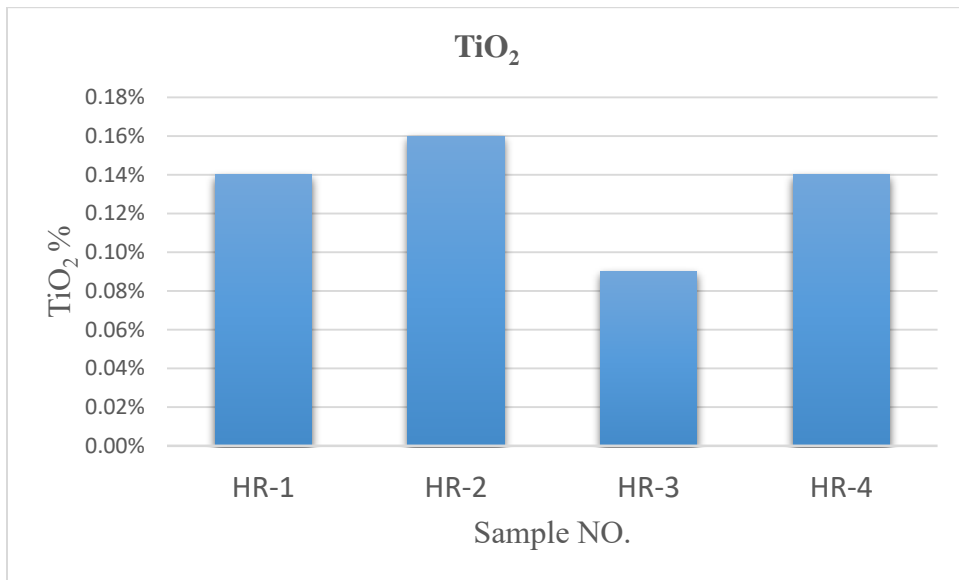


Fig 4.16 Graphical comparison of TiO₂ in the collected rock samples of Habib Rahi Formation.

4.6 Alkali-silica reaction

The alkali-silica reaction (ASR) is a chemical reaction that can take place in concrete structures and result in the formation of a gel-like substance within the concrete. Over time, this gel may cause the concrete to expand and crack, potentially risking the structural integrity of the affected elements (Monnin, 2006). This test method enables the detection of a potentially harmful Alkali-Silica Reaction in aggregate in mortar bars within 16 days.

Apparatus

- Sieves
- Mixer, Paddle, and Mixing Bow
- Containers
- Containers

Reagents

- Sodium Hydroxide (NaOH)
- Sodium Hydroxide Solution

Procedure

Initial storage and reading immediately after filling the moulds, place them in the wet cabinet or room. Specimens must be held in the moulds for 24 ± 2 hours. While the specimens must be protected from moisture loss, remove them from the moulds and appropriately identify and calculate an initial reading. Record the initial and all subsequent values to the closest 0.002 millimetres. Put the specimens made with each aggregate sample in a storage container with enough tap water to cover them and place in an oven or water bath at $80.0 \pm 2.0^\circ\text{C}$ ($176 \pm 3.6^\circ\text{F}$) for 24 hours.

Remove the containers at a time from the oven or water bath. After the bars in the first container have been measured and returned to the oven or water bath, remove the other containers. Taking each bar out of the water one at a time, thoroughly dry its surface with a towel, giving careful attention to the two metal gauge studs. Take the zero reading of each bar just after drying and read it instantly as the bar is in position. Complete the drying and reading process within 15 ± 5 seconds after withdrawing the specimen

from the water. After taking the readings, place the specimen on a towel and wait until the other bars have received measurable values. Place all of the specimens created from each aggregate sample in a container with enough 1N NaOH to completely submerge them, at a temperature of 80.0 ± 2.0 °C (176 ± 3.6 °F). Return the container to the water bath or oven after sealing it.

For 14 days after the zero reading, take periodic comparator readings of the samples with at least three intermediate values at roughly the same time each day. Take at least one reading per week if the readings are continued after the initial 14-day period. With the exception of returning the samples to their own container after measurement, the technique is the same as that detailed in the section on zero readings.

Calculate the difference between the specimen zero measurable reading at each period to the nearest 0.001% of the effective gauge length and record it as the specimen's expansion for that period. As the expansion for a given duration, report the average expansion of three specimens of a specified cement-aggregate combination to the closest 0.01%.

Chapter #5

Geotechnical Analysis

5.1 Physical Test

Limestone is a typical rock that generally appears in thick beds that are structurally straightforward and simple to quarry. Certain physical characteristics of the limestone must always be taken into account when evaluating it for multiple applications. When evaluating a material for use as an aggregate source, its physical strength, are important factors. Following is a detailed description of the various standard aggregate tests performed on aggregate samples from the Habib Rahi Formation.

5.1.1 Sieve Analysis for Coarse Aggregate

All aggregate technicians are required to pass the sieve analysis test, often known as the gradation test. The distribution of aggregate particles, by size, inside a given sample is established by the sieve analysis in order to evaluate compliance with design, production control requirements, and verification criteria. When used in conjunction with other tests, the sieve analysis is an extremely effective quality control as well as acceptance tool.

Apparatus

- Balance
- Sieves
- Oven dry machine

Procedure

AASHTO T 248 requires that samples be collected in the field and sized for testing. In an oven preheated to 230 ± 9 °F (110 ± 5 °C), in an electric skillet, or over an open flame, samples are dried to a consistent weight. By multiplying the sample's overall weight, weigh the sample to the closest 0.1 g. After the sample has been graded, the loss of any material will be checked using this weight. According to the specifications, choose acceptable sieve sizes. Once the sample has been sufficiently stirred and shaken, the sieves should be nested in decreasing size order from top to bottom.

Table 5.1 Tabular presentation of sieve analysis of coarse aggregate.

SIEVE ANALYSIS FOR COARSE AGGREGATE AASHTO (T-27/T-88)				
Initial Wt. Of Dry Sample		Wt. of Dry Sample after		
gram		5176.0	washing	
ASTM Sieve No.	Size (mm)	Cumulative Wt. Of Retained (g)	Percent of Retained (%)	Percent of Passing (%)
1" ½	38.0	Nil	0.0	100.0
1"	25.0	2088	40.3	59.7
¾"	19.0	3818	73.8	26.2
½"	12.5	4538	87.7	12.3
⅜"	9.50	4639	89.6	10.4
4	4.75	5134	99.2	0.8

5.1.2 Specific Gravity and Water Absorption

In several mixtures containing aggregate, such as Portland cement concrete, bituminous concrete, and other combination that are proportioned or analyzed on an absolute volume basis, relative density (specific gravity) is the characteristic that is usually utilized to calculate the volume occupied by the aggregate. Relative density (specific gravity) is utilized as well in Test Method C 29/C 29M to determine aggregate voids. . If the aggregate is wet, or if its absorption needs have been met, relative density (specific gravity) (SSD) is used.

Conversely, when the aggregate is dry or is thought to be dry, the relative density (specific gravity) (OD) is used for calculations. When it is determined that the aggregate has been in contact with water for long enough to satisfy the majority of the absorption potential, absorption values are used to calculate the change in mass of an aggregate due to water absorbed in the pore spaces within the constituent particles, as compared to the dry condition.

The laboratory standard for absorption is the outcome of submerging dry aggregate for a set amount of time. Aggregates mined under the water table frequently have a moisture content that exceeds the absorption measured by this test method if used without being given time to dry before use. On the other hand, some aggregates may still retain some absorbed moisture within 24 hours after being soaked if they are not continuously kept moist until they are used.

Table 5.2 Result of water absorption specific gravity and porosity of different rock samples

	Sample No.	HR-1	HR-2	HR-3	HR-4	
A	Wt. of oven Dry Sample In Air (g)	1420.0	1420.0	1420.0	1420.0	Average
B	Wt. Of Saturated surface dry sample in air (g)	1460	1450	1456	1456	
C	Wt. Of Saturated surface dry sample in water (g)	839.0	845.0	832.0	839	
D	SSD Volume g/cc	621.0	605.0	624.0	617.0	
E	Dry Volume g/cc	581.0	575.0	588.0	582.0	
F	Oven Dry Bulk Specific Gravity (a)/(b-c)	2.287	2.347	2.276	2.303	2.309
G	SSD Bulk Specific Gravity (b)/(b-c)	2.351	2.397	2.333	2.360	2.363
H	Apparent Specific Gravity (a)/(a-c)	2.444	2.470	2.415	2.442	2.442
F	Absorption b % = $\{(b-a)/a\} \times 100$	2.82	2.11	2.54	2.53	2.37

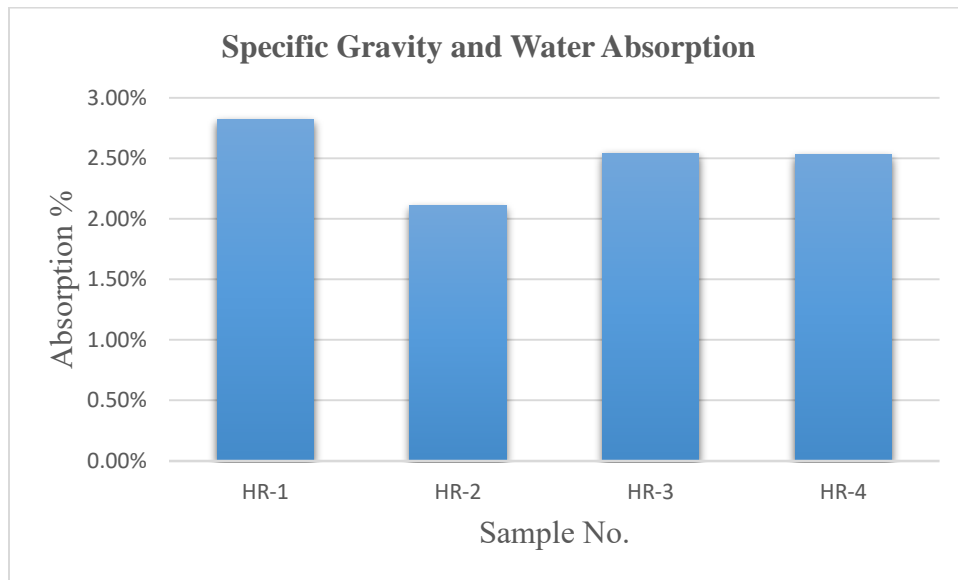


Fig 5.1 Graphical representation of Specific Gravity and Water absorption.

5.1.3 Particles shape (Flakiness and elongation)

This test method can be used to determine the proportions of flat particles, elongated particles, or flat and elongated particles in coarse aggregates. To calculate the ratios of width to thickness, length to width, or length to thickness, individual aggregate particles of particular sieve sizes are measured. This

test method offers a way to determine the relative shape properties of coarse aggregates or to verify compliance with specifications that restrict such particles.

Apparatus

- Proportional Caliper Device
- Verification of Ratio
- Balance

Procedure

If a mass measurement is necessary, oven-dry the sample to a consistent mass at 230 ± 9 °F (110 ± 5 °C). Drying is not required for particle count determination. Using Test Method C-136, sieve the sample that will be put through the test. Reduce each size fraction present in the amount of 10% or more of the original sample in accordance with Practice C 702 until approximately 100 particles are obtained for each size fraction required, using the material retained on the 9.5 mm (3/8 in.) or 4.75 mm (No. 4), as required by the specification being used..

Test each particle in each size fraction to determine whether it is flat, elongated, or neither flat nor elongated, then categorize the results into one of three categories. Use the proportional caliper tool as shown below, with the appropriate ratio set.

Flat Particle Test: Set the larger opening equal to the particle width. The particle is flat if the thickness can be placed in the smaller opening.

Elongated Particle Test: Set the larger opening equal to the particle length. The particle is elongated if its width can be placed within the smaller opening. After the particles have been classified into group, determine the proportion of the sample in each group by either count or mass, as required.

Flat and Elongated Particle Test: Test each of the particles in each size fraction and place them in one of two groups: (1) flat and elongated or (2) not flat and elongated, Use the proportional caliper device

Test for Flat and Elongated Particles: Sort the particles into one of two groups after testing each particle in each size fraction: Flat and elongated make use of the proportional caliper. Setting the larger opening at the particle's length is a measurement. If the particle can completely fit through the caliper's smaller opening when it is positioned to measure thickness, it is flat and elongated.

Table 5.3 Flakiness and elongation test values for the aggregate of Habib Rahi formation

Sample No.	Size of Aggregate		Original Gradation	Weight of Test Fraction	Weight of Thin And Elongated Particles	Thin and Elongated Particles in %	Corrected Avg. Weight %
	Passing through sieve	Retained on sieve					
HR-1			A	B	C	D	
	1-1/2"	1"	25.4	3000	126	4.2	1.0668
	1"	3/4"	24.2	2000	147	7.35	1.7787
	3/4"	1/2"	24.8	1500	89	5.93333333 3	1.471467
	1/2"	3/8"	9.1	1000	72	7.2	0.6552
	3/8"	1/4"	16.5	500	35	7	1.155
	Total		100				6.127167
HR-2	1-1/2"	1"	25.4	3000	130	4.33333333 3	1.100667
	1"	3/4"	24.2	2000	140	7	1.694
	3/4"	1/2"	24.8	1500	95	6.33333333 3	1.570667
	1/2"	3/8"	9.1	1000	75	7.5	0.6825
	3/8"	1/4"	16.5	500	40	8	1.32
	Total		100				6.367833
HR-3	1-1/2"	1"	25.4	3000	125	4.16666666 7	1.058333
	1"	3/4"	24.2	2000	130	6.5	1.573
	3/4"	1/2"	24.8	1500	80	5.33333333 3	1.322667

	1/2"	3/8"	9.1	1000	65	6.5	0.5915
	3/8"	1/4"	16.5	500	30	6	0.99
	Total		100				5.5355
HR-4	1-1/2"	1"	25.4	3000	145	4.8333333 3	1.227667
	1"	3/4"	24.2	2000	128	6.4	1.5488
	3/4"	1/2"	24.8	1500	62	4.1333333 3	1.025067
	1/2"	3/8"	9.1	1000	61	6.1	0.5551
	3/8"	1/4"	16.5	500	38	7.6	1.254
	Total		100				

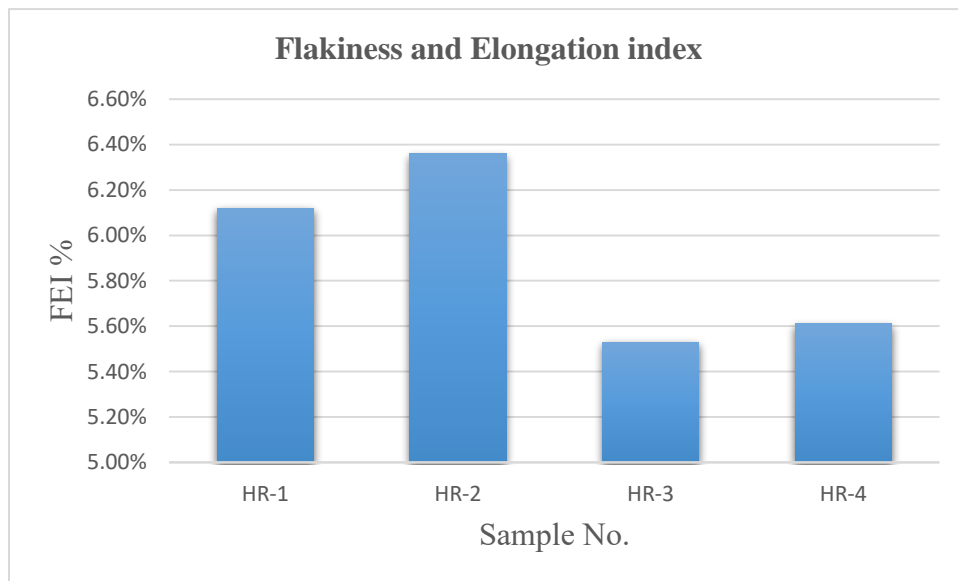


Fig 5.2 Graphical representation of Flakiness and Elongation index.

5.2 Durability Test

5.2.1 Loss Angeles Test

The Los Angeles laboratory instruments can be used to assess the resistance to degradation of coarse aggregate sizes smaller than 37.5 mm (1 1/2 inch) using the test procedure described below.

Apparatus

- Los Angeles Machine
- Sieves
- Balance
- Steel balls

Procedure

In the Los Angeles testing device, insert the test sample and the charge. Rotate the instrument for 500 revolutions at a speed of 30 to 33 revolutions per minute. After the requisite number of rotations, remove the material from the machine, then separate the sample using a sieve with a mesh size more than 1.70 mm. In line with Test Method C 136, the finer portion should be sifted through a 1.70-mm sieve. Clean the material that has a particle size coarser than the 1.70-mm (No. 12) sieve, oven-dry it at 110 °C (230 °F), and then weigh the remaining aggregate to obtain the mass to the nearest 1 g.

Table 5.4 Loss Angeles test for Habib Rahi formation

Sieve Size		Weight and Grading of Test Sample (gm)				Aggregate Weight used (gm)				
Passing	Retained	A	B	C	D	Sample No.				Ave.
						HR-1	HR-2	HR-3	HR-4	
1 1/2 inch	1 inch	1250±25	---	---	---	1250	1250	1250	1250	
1 inch	3/4 inch	1250±25	---	---	---	1250	1250	1250	1250	
3/4 inch	1/2 inch	1250±10	2500±10	---	---	1250	1250	1250	1250	
1/2 inch	3/8 inch	1250±10	2500±10	---	---	1250	1250	1250	1250	
3/8 inch	1/4 inch	---	---	2500±10	---	---	---	---	---	
1/4 inch	No. 4	---	---	2500±10	---	---	---	---	---	
No. 4	No. 8	---	---		5000±10	---	---	---	---	
Total Weight (X)		5000±10	5000±10	5000±10	5000±10	5000	5000	5000	5000	
Weight of Sample After Test Retained No.12 Sieve (Y)						3545	3565	3512	3645	
Weight of Sample After Test Passing No.12 Sieve Z=(X-Y)						1455	1435	1488	1355	
Percentage Loss by Abrasion (%) (Z/X)*100						29.1	28.7	29.8	27.1	28.6
Max. Allowable Percentage Loss										

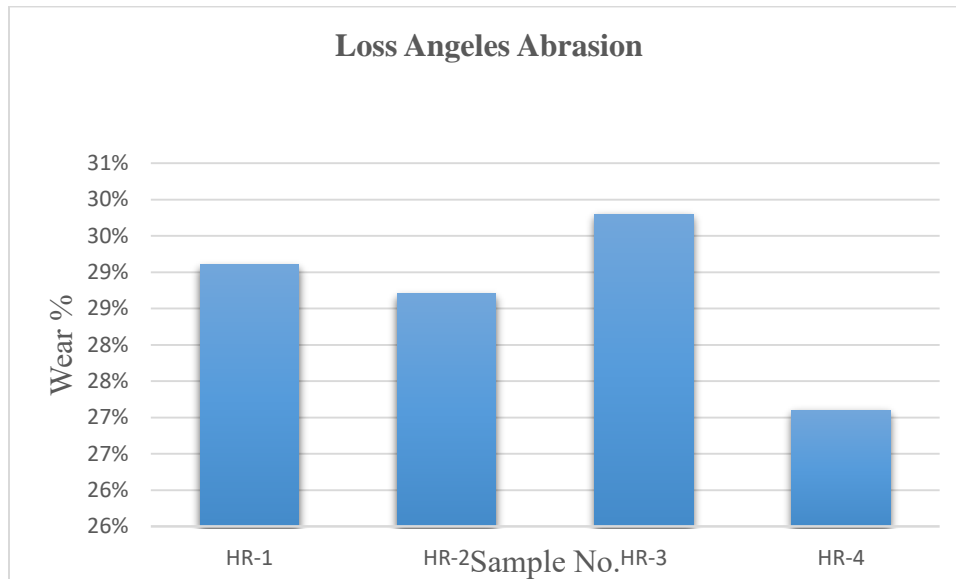


Fig 5.3 Graphical representation of Loss in weight samples.

5.2.2 Soundness Test

The process for determining an initial evaluation of an aggregate's soundness for utilization in concrete and other applications is described in this test method. The outcomes can be contrasted with specifications, such as Specification C 33, designed to determine whether an aggregate is appropriate for a certain application.

Apparatus

- Sieves
- Containers
- Balances
- Drying Oven
- Specific Gravity Measurement
- Special Solutions Required {(Sodium sulfate) (Barium Chloride Solution)}

Procedure

The samples should be submerged in the sodium sulfate solution for at least 16 hours but no longer than 18 hours, making sure the solution covers them completely. Cover the containers during the immersion period and maintain the samples submerged in the solution at a temperature of $70\pm 2^{\circ}\text{F}$ ($21\pm 1^{\circ}\text{C}$) to decrease evaporation and prevent unintended inclusion of extraneous substances.

When the time for immersion is over, take the aggregate sample out of the solution, let it drain for 15 minutes, and then place it in the drying oven. Temperature for soundness $230\pm 9^{\circ}\text{F}$ ($110\pm 5^{\circ}\text{C}$) must have previously been attained in the oven. Dry the samples until the weight is constant at the recommended temperature. Drying success will be considered to have been accomplished if there is a weight loss of less than 0.1% of the sample weight after 4 hours. Once consistent weight has been attained, let the samples cool to room temperature before re-immersing them in the prepared solution. So until the necessary number of cycles is reached, repeat the process of alternate immersion and drying.

Following the completion of the final cycle and after the sample has cooled, wash the sample to remove any sodium sulfate, as indicated by the reaction of the wash water with barium chloride (BaCl_2). Run water through the samples' containers at $110\pm 10^{\circ}\text{F}$ (43°C) to clean them. In order to do this, they can be placed in a tank where hot water can be poured in towards the bottom and allowed to overflow. During

the washing procedure, the samples must not be touched or exposed to anything abrasive as this could break up the particles.

Table 5.5 Gradation of aggregate and their weights for soundness test of Habib Rahi formation.

Sample No.	Passing Through Sieve	Retained Through Sieve	Original Grading %	Wt. of Fraction Before Test (g)	Wt. Test Fraction After Test (g)	Loss in wt. after Test	Actual Loss %	Corrected Average Weight Loss %
			(A)	(B)	(C)	D=(B-C)	E=(D/B)100	F=(A*E)/100
HR-1	2-1/2"	1-1/2"	-	-	-	-	-	-
	1-1/2"	1"	40.34	985	957.6	27.4	2.8	1.12
	1"	3/4"	33.4	515	462.3	52.7	10.2	3.42
	3/4"	1/2"	13.9	660	645.3	14.7	2.2	0.31
	1/2"	3/8"	1.8	330	316.1	13.9	4.2	0.08
	3/8"	#4	10.1	300	272.8	27.2	9.1	0.92
Total			100	Total Loss %				5.84
HR-2	2-1/2"	1-1/2"	-	-	-	-	-	-
	1-1/2"	1"	40.34	990.8	962.2	28.6	2.9	1.16
	1"	3/4"	33.4	521.7	476.2	45.5	8.7	2.91
	3/4"	1/2"	13.9	667	642.3	24.7	3.7	0.51
	1/2"	3/8"	1.8	334	317.5	16.5	4.9	0.09
	3/8"	#4	10.1	298.7	274.1	24.6	8.2	0.83
Total			100	Total Loss %				5.515
HR-3	2-1/2"	1-1/2"	-	-	-	-	-	-
	1-1/2"	1"	40.34	995.4	965.1	30.3	3.0	1.23
	1"	3/4"	33.4	522.6	473.3	49.3	9.4	3.15
	3/4"	1/2"	13.9	670	642.3	27.7	4.1	0.57
	1/2"	3/8"	1.8	345	317.5	27.5	8.0	0.14
	3/8"	#4	10.1	300	278.5	21.5	7.2	0.73
Total			100	Total Loss %				5.823
HR-4	2-1/2"	1-1/2"	-	-	-	-	-	-
	1-1/2"	1"	40.34	1000	970.0	30.0	3.0	1.21
	1"	3/4"	33.4	530	475.6	54.4	10.3	3.43
	3/4"	1/2"	13.9	680	650.3	29.7	4.4	0.61
	1/2"	3/8"	1.8	350	321.9	28.1	8.0	0.14
	3/8"	#4	10.1	295	280.7	14.3	4.8	0.49
Total			100	Total Loss %				5.881

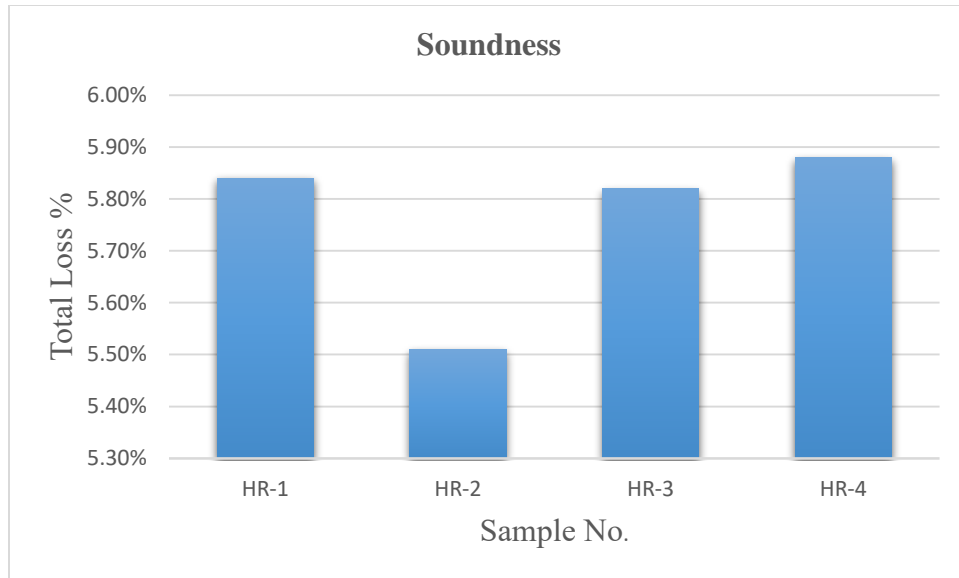


Fig 5.4 Graphical representation of soundness test

5.3 Mechanical test

5.3.1 Aggregate Impact Value

Using the procedures outlined in this section of BS 812, the aggregate impact value (AIV), which offers an alternative measurement of an aggregate's resistance to a sudden shock or impact, is calculated.

Apparatus

- Impact testing machine
- Sieves
- A tamping rod
- A balance
- A well-ventilated oven,
- A rubber mallet
- A metal tray.
- A brush.

Procedure

Reduce the laboratory sample to a test portion with an amount of mass sufficient to produce three test specimens with sizes ranging from 14 mm to 10 mm. Completely filter the entire surface dry test piece through the 14 mm and 10 mm test sieves to remove the oversize and undersize fractions. Divide the

resulting 14 mm to 10 mm portion to obtain three test specimens, each having sufficient mass to fill the measure when it is filled following the procedure described subsequently.

Dry the test specimen by heating it for no longer than 4 hours at a temperature of 105.5 °C. Before testing, allow to cool to room temperature. Using a scoop, completely fill the measure with the aggregate that makes up the test specimen with the rounded end of the tamping rod, tamp the aggregate with 25 equally spaced strokes. The tamping rod is dropped freely from a height of approximately 50 mm above the aggregate surface to deliver each blow. To remove any surplus aggregate, empty the container by bringing the tamping rod across and in touch with the top of the container. Manually remove any aggregate in the way, and fill up any obvious depressions with additional aggregate. For the second test specimen, use the same mass, and record the aggregate's net mass in the measure.

Place the impact machine on a level plate, block, or floor, resting it there without packing it down to make sure it is rigid and that the hammer guide columns are vertical. Before connecting the impact machine, place the entire test specimen in the cup and compact it using 25 strokes of the tamping rod. In order to disrupt the test specimen as little as possible, fix the container firmly to the machine's base. In the cup, place the aggregate so that the bottom face of the hammer is 380.5 mm above the top surface. Then, just let the hammer fall naturally onto the aggregate. 15 of these blows, spaced no closer than 1 second apart, should be given to the test object in total.

Holding the cup over a clean tray, tap it on the outside with a rubber mallet until the particles are sufficiently disturbed up to allow the substance of the specimen to drop freely into the tray. This will remove the crushed aggregate. Transfer any tiny particles adhering to the interior of the cup and the interior of the hammer to the tray using the stiff bristle brush. Weigh the container and the aggregate, and record the used aggregate's mass (W1) down to the closest 0.1 g.

Use a 2.36 mm test sieve to sift the test sample hole in the tray until no more substantial amount passes after another minute. A further specimen should be tested if the total mass (W2 + W3) deviates from the initial mass (W1) by more than 1 g. Weigh and record the masses of the fractions passing and kept on the sieve (W2 and W3, respectively) to the nearest 0.1 g.

$$\text{Aggregate Impact Value (AIV)} = W2 / W1 \times 100$$

Table 5.6 Impact value test results for the limestone sample of Habib Rahi formation.

Sample No.	HR-1	HR-2	HR-3	HR-4	Average Value
Oven dry samples W1	500	500	500	500	
Weight of aggregate before test	373	367	376	380	
Weight of aggregate passing 2.36 mm sieve W2	127	133	124	120	
% Impact value (Wf) = $W2/W1 * 100$	25.4%	26.6%	24.4%	24%	25.1%

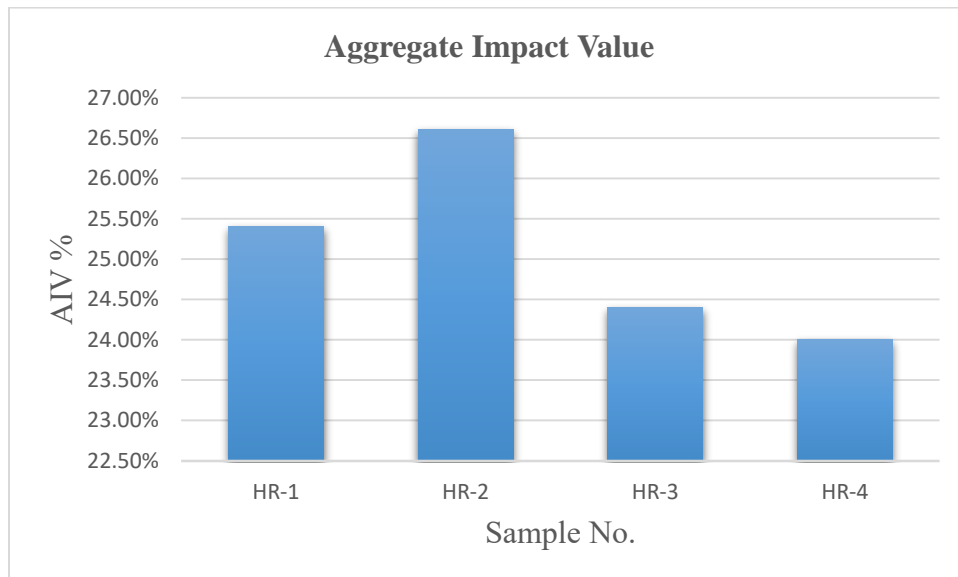


Fig 5.5 Graphical representation of Aggregate Impact Value.

5.3.2 Aggregate Crushing Value

The aggregate crushing value test on coarse aggregates provides an approximate measure of the resistance of an aggregate crushing with a gradually applied compressive stress. The coarse aggregate crushing value is the proportion of crushed particles that results when test aggregates are subjected to a particular load under defined conditions.

Apparatus

- A Steel cylinder
- A tamping rod
- Weight Balance
- Sieves
- Oven dry machine
- A compression test machine

Procedure

Weigh the cylinder (W) by setting it on the base plate. Three layers of the sample should be applied, with 25 tamping rod strokes between each layer. It is important to exercise caution when utilizing weak materials to prevent fracturing the particles and weigh them (W1) Insert the plunger so that it sits on top of the surface after carefully leveling the aggregate surface. The plunger is being carefully watched to make sure it doesn't get stuck in the cylinder. On the loading platform of the compression testing device, place the cylinder with the plunger. Applying a consistent rate of load will enable a 40T total load to be applied in 10 minutes. Remove the material from the cylinder and let go of the load. To prevent losing fines, carefully sieve the material through a 2.36mm IS sieve. Weigh the portion (W2) that passes through the IS sieve. The weight of produced fines in each test shall be represented as a percentage of the weight of the entire sample, with the result being recorded to the closest whole number.

Table 5.7 Crushing value test for the aggregate of Habib Rahi formation.

Sample No.	HR-1	HR-2	HR-3	HR-4	Average Value
Weight of aggregate before test W1	1200	1190	1200	1180	
Weight of aggregate passing 2.36 mm sieve W2	303	306	312	295	
% Crushing Value (Wf) = $W2/W1*100$	25.24%	25.71%	26%	25%	25.4%

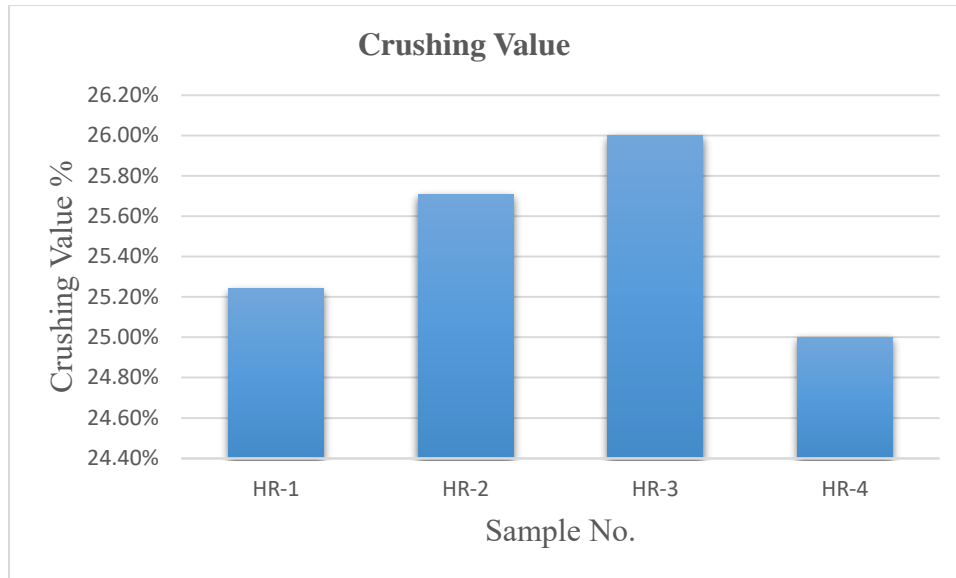


Fig 5.6 Graphical representation of Crushing Value

5.3.3 Unit Weight

Apparatus

- Balance
- Tamping rod
- Measures
- Scoop
- Calibration Equipment

Procedure

Take the sample as per Practice D 75, and decrease it to the test sample size as per Practice C 702.

7.1. The size of the sample shall be approximately 125 to 200 % of the quantity required to fill the measure, and shall be handled in a manner to avoid segregation. Dry the aggregate sample to essentially constant mass, preferably in an oven at $230 \pm 9^{\circ}\text{F}$ [$110 \pm 5^{\circ}\text{C}$]. Fill the measure with water at room temperature and cover with a piece of plate glass in such a way as to eliminate bubbles and excess water. By dividing the mass of water needed to fill the measure by its density, you may get its volume, or V . Alternately, you can determine the factor for the measurement to be taken ($1/V$) by dividing the water's density by the mass needed to fill it.

Only when clearly stated, the loose bulk density shoveling approach must be applied. Otherwise, the rodding process for aggregates with a nominal maximum size of 112 in. [37.5 mm] or less, or the jiggling procedure for aggregates with a nominal maximum size more than 112 in. [37.5 mm] but not exceeding 5 in. [125 mm], shall be used to calculate the compact bulk density.

Rodding Procedure

Next fill the measure, then use your fingertips to smooth the top. With 25 regularly spaced strokes of the tamping rod, flatten the layer of aggregate. Completely fill the measure, level it again, and rod it as before. Finally, fill the container to the maximum and rod it once again as described earlier. With your fingers or a straightedge, level the aggregate's surface so that any small edges from the larger pieces of coarse aggregate roughly balance the larger voids in the surface beneath the top of the measure.

Don't allow the rod to strike the bottom of the measure when rodding the first layer. Use a lot of force when tamping the second and third layers of aggregate, but only enough to push the tamping rod through the top layer of aggregate.

Jiggling Procedure

Fill the container in approximately three equal layers, compacting each layer by placing the container on a hard foundation, like a cement-concrete floor. Alternate between raising the opposite sides by about 2 inches (50 mm) each time and allowing the container to descend, delivering a sharp, slapping blow. By this process, the aggregate particles will arrange themselves into a densely compacted form. Compact each layer by performing 50 repetitions of the described method, evenly distributed with 25 repetitions on each side. Level aggregate surface with your fingers or a straightedge in such a way that any slight projections of the larger pieces of the coarse aggregate roughly balance the larger voids in the surface below the top of the measure. Determine the mass of the measure plus its contents, as well as the mass of the measure alone, and note the results to the closest 0.1 pound [0.05 kilogramme].

Shoveling Procedure

Fill the measure to the brim with a shovel or scoop, discharging the aggregate from a height not to exceed 2 inches. [50 millimetres] above the measure's top. Take care to avoid segregation of the particle sizes of which the sample is composed. Level the aggregate surface with the fingers or a straightedge so that any slight projections of the larger pieces of the coarse aggregate roughly balance the larger voids in

the surface below measure's top. Determine the mass of the measure plus its contents, as well as the mass of the measure alone, and round up to the nearest 0.1 pound [0.05 kilograms].

Table 5.8 Unit weight result for the Habib Rahi formation.

Sample No.	Wt. of mold.(g)	Volume of mold(cm)	Wt. of mold + aggregate (gm)	Wt. of aggregate	Bulk unit wt. (g/cm ³)	Average
HR-1	2238	9515	14700	12462	1.309721492	1.296584341
HR-2	2238	9515	14570	12332	1.296058854	
HR-3	2238	9515	14500	12262	1.288702049	
HR-4	2238	9515	14530	12292	1.291854966	

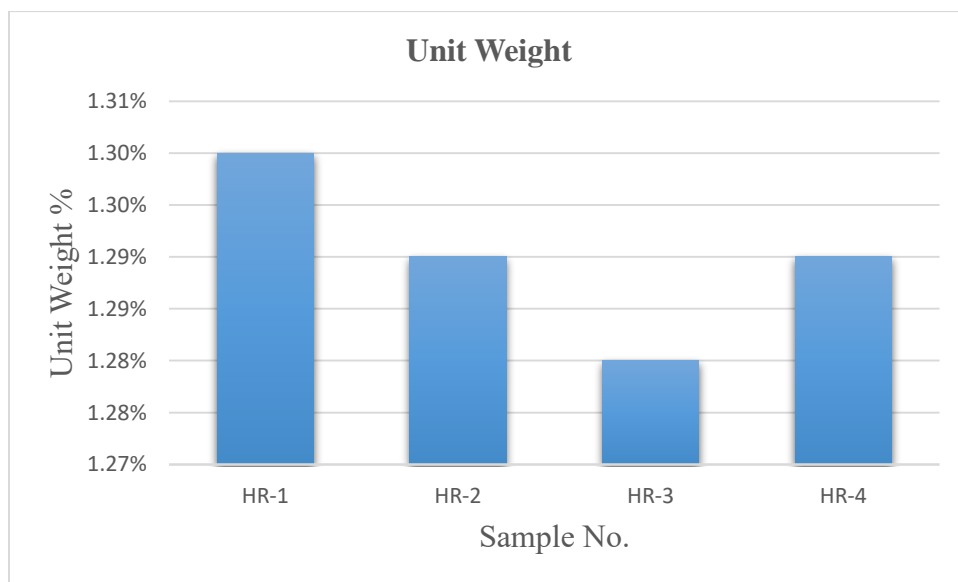


Fig 5.7 Graphical representation of unit weight

5.4 Bituminous test

5.4.1 Coating and Striping

Apparatus

- Container
- Scales
- Spatula
- Constant Temperature Oven
- Sieves

Procedure

For Tar and Cutback Asphalts Coated Dry Aggregate. Coating Put 100 ± 1 g of room-temperature, oven-dry aggregate into the mixing container. Depending on the quality of bituminous material, add 5.5 ± 0.2 g, of bituminous material to the temperature indicated, and aggregate vigorously with the spatula for two minutes.

Cure the coated aggregate for two hours at $60\text{ }^{\circ}\text{C}$ ($145\text{ }^{\circ}\text{F}$) in the original container. During this curing process, the oven's ventilation port should be left open. After curing, stir the mixture with a spatula until the bituminous material stops dripping off the aggregate, or until the mixture reaches room temperature. After remixing, the coating must be complete, with no bare patches. The coated aggregate needs to be transferred to a 600 ml glass container. 400 mL of distilled water at room temperature added as soon as possible. For 16 to 18 hours, let the coated aggregate soak in the water. Estimating the coated area visually during a striping test without stirring or disrupting the coated aggregate and removing any floating film. By seeing through the water, it was possible to determine whether more than 95% of the aggregate's total visible area was covered in leftovers. Any thin, transparent, brownish regions are to be regarded as fully covered.

Table 5.9 Bitumen test for the aggregate of Habib Rahi formation.

Bitumen Aggregate Mixture				
• Size of Aggregate	9.5/6.3 mm			
• Weight of Aggregate	200 gm			
• Weight of Bitumen	5 %			
Heating and Mixing				
• Container and Aggregate	135-149 C for 1 hour in Oven			
• Asphalt	Heat separately to 135/149 C			
• Maxing with warm spatula	for 2-3 minutes till the result			
• Cooling	Allow the mix to cool at room temp			
Curing in Distilled Water				
• Quantity of Water	400 ml			
• Temperature	25 C			
• Duration	16-18 hrs			
Sample No.	HR-1	HR-2	HR-3	HR-4
Weight of material	200 gm	200 gm	200 gm	200 gm
Bitumen grade (60-70)	10%	10%	10%	10%
Water immersion at 25 c	18 hrs	18 hrs	18 hrs	18 hrs
Visual inspection coated area	92%	91%	95%	93%
Specification	Estimated coated area (Above 90%)			

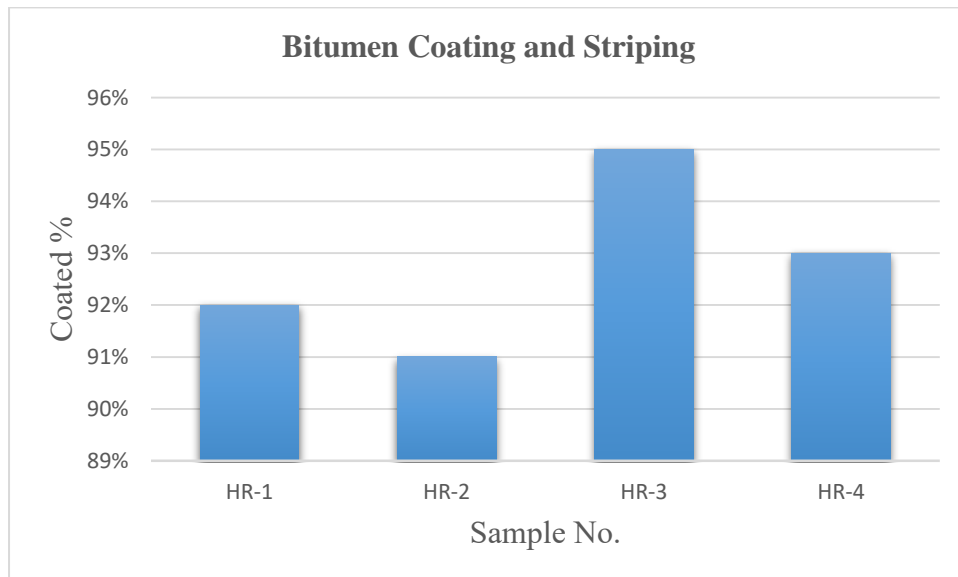


Fig 5.8 Graphical representation of bitumen test.

CHAPTER #6

Results, Conclusion and Recommendation

In past construction projects, coarse aggregates have played a crucial role in providing strength, stability, and durability to various types of structures and infrastructure. These aggregates, typically consisting of crushed stone, gravel, or other natural materials, has been extensively utilized in concrete, asphalt, and other construction materials. The comprehensive study conducted on the rock aggregate suitability of the Habib Rahi Formation in Zindapir anticline, Dera Ghazi Khan, Pakistan, provides valuable insights into the potential utilization of coarse aggregate for construction and infrastructure development. The purpose of the study was to evaluate the rock aggregates' petrographic, geotechnical, and chemical characteristics as well as their specification for various construction uses.

6.1 Results

According to the Dunham classification scheme of carbonates, the petrographic investigation conducted according to ASTM C-295 revealed that the Habib Rahi Formation limestone of the study region mainly consists of Mudstone to Wackestone depositional fabric. From petrographic perspective the Habib Rahi Formation limestone is dominantly composed of calcite and bioclast. The major mineral phases include CaO (48.7%), SiO₂ (5.6%), Al₂O₃ (1.2%), Fe₂O₃ (1.2%), K₂O (0.2%), and TiO₂ (0.1%) are the principal oxides that are present in the examined Habib Rahi limestone according to the average XRF geochemical concentration. Moreover, the XRF elemental analysis reveals that the primary elements identified by the specimen's results are Ca, Si, Fe, Al, K, and Ti. The geochemistry analysis shows that Habib Rahi Formation has no reactive constituents. Alkali-silica reaction tests were done in accordance with (ASTM C 1260) also reveals that the Habib Rahi Formation limestone has expansion of less than (0.1%) indicating safe nature.

Sieve analysis Specific gravity and water absorption test, Flakiness and Elongation test, Loss Angeles abrasion test, Soundness test, Aggregate Impact value test, Aggregate Crushing value test, Unit weight test, and Coating and Striping for Coarse aggregate were among the physical tests conducted. According to ASTM standard, sieve analysis of coarse aggregate is within the prescribed parameters. Within ASTM standard limitations, the range of specific gravity, and water absorption values is (2.5%). The bulk SSD specific gravity and the bulk oven dried specific gravity are both taken into account. For bulk oven-dried specific gravity, the values are 2.309, while for bulk SSD specific gravity, they are 2.363, both values falling within the ASTM standard limits. Flakiness and Elongation test were conducted in accordance to

specified standard. The results for the Habib Rahi Formation for Flakiness and Elongation Index are (5.905) and its falls within the specified standard limit. The Loss Angeles Abrasion test tracks the deterioration of aggregate producing rocks. In order to pass the abrasion test, the maximum value for the limestone must be less then (40%), and the result is (28.675%) which falls within the specified standard limit.

In this research project, soundness test were conducted according to ASTM for coarse aggregate, the standard allowed limit is (12%), and the result for soundness is (5.7%), which falls within the desirable limit. The aggregate impact value result for the Habib Rahi limestone is (25%), and the maximum allowed limit is (30%). The aggregate crushing value tests results are (25.4%) and the maximum allowed limit is (30%), which fells with the specified limit accordance to ASTM. According to ASTM norms, a bulk density test was conducted and the results are (1.29 MT) and the maximum allowed limit is (1.5 MT). After coating and stripping of bitumen, the result for coating of the Habib Rahi Formation Limestone covers greater than (90%) of the sample, which falls within the specified limit.

6.2 Conclusion

- In the current research work, the potential of coarse aggregate suitability studies of Habib Rahi limestone of Zindapir Anticline was investigated through a range of physical, mechanical, and chemical tests.
- In the study area, the Habib Rahi Formation, limestone was investigated on the basis of petrographic and geochemical tests, suggesting that it has no reactive constituents. According to Dunham Classification Scheme for carbonates Habib Rahi Formation is Mudstone-wackestone depositional fabrics.
- All aggregate strength limits, comprising LAAV, AIV, and ACV, Soundness have been determined to be within the accepted range with accordance to ASTM, AASHTO, and BS.
- The Habib Rahi Formation meets all engineering criteria and is comparable to AASHTO, ASTM, and BS standards, limestone of Zindapir Anticline, Dera Ghazi Khan, Pakistan, is the potential aggregate source.

Recommendation

- It is strongly advised to use the Habib Rahi limestone aggregate for road surfacing because it shown great bitumen affinity.
- Habib Rahi limestone aggregate falls under the specification of normal weight aggregate. Thus, it can be argued that limestone from Habib Rahi is acceptable for utilization as coarse aggregate in construction projects.
- Additionally, it is appropriate for usage as aggregate subbase, aggregate base coarse, and asphaltic base coarse material in the construction of roads.

References

- AASHTO T 85, (2014). Standard Method of Testing for Specific gravity and absorption of coarse aggregate. The American Association of State Highway and Transportation Officials, Washington, United States.
- AASHTO, (2014). Standard specifications for transportation materials and methods of sampling and testing. AASHTO
- AASHTO, T. (2002). 182, Standard method of test for coating and stripping of bitumen-aggregate mixtures. AASHTO Standards, Washington DC (84.
- AASHTO-T-104-99. (2007). Standard method of test for soundness of aggregate by use of sodium sulfate or magnesium sulfate. The American Association of State Highway and Transportation Officials, Washington, United States.
- Afzal, J., Kuffner, T., Rahman, A., & Ibrahim, M. (2009, November). Seismic and well-log based sequence stratigraphy of the early Cretaceous, Lower Goru “C” sand of the Sawan gas field, middle Indus Platform, Pakistan. In Proceedings, Society of Petroleum Engineers (SPE)/Pakistan Association of Petroleum Geoscientists (PAPG) Annual Technical Conference, Islamabad, Pakistan.
- Ahmed, R., & Ali, S. M. (1991). Tectonic and structural development of the eastern part of Kirthar Fold Belt and its hydrocarbon prospects. *Pakistan Journal of Hydrocarbon Research*, 3(2), 1931.
- Ahsan, N., & Gondal, M. M. I. (2016). Aggregate suitability studies of limestone outcrops in Dhak pass, western Salt range, Pakistan. *International Journal of Agriculture and Applied Sciences (Pakistan)*.
- Ali, S. M., Ahmed, J., & Ahmed, R. (1995). Evidence of wrench tectonics in the Sulaiman Fold Belt. In Pakistan and its implication for hydrocarbon prospects: Abstract and Paper presented in Second South Asian Geological Congress, Colombo, Sri-Lanka.
- ASTM D75-87. (1992). Standard practice for sampling aggregates. ASTM International, Pennsylvania, United States.

- ASTM, C. (2003). 125 Standard terminology relating to concrete and concrete aggregates. Annual Book of ASTM Standards, 4, 23.
- ASTM, C. (2006). 131. Standard Test Method for Resistance to Degradation of Small-Size Coarse Aggregate by Abrasion and Impact in the Los Angeles Machine. Conshohoken, PA: ASTM.
- Baker, M. A., & Jackson, R. O. (1964). Geological Map of Pakistan 1: 2,000,000: Geological Survey of Pakistan.
- Banks, C. J., & Warburton, J. (1986). 'Passive-roof' duplex geometry in the frontal structures of the Kirthar and Sulaiman Mountain belts, Pakistan. *Journal of structural Geology*, 8(3-4), 229-237.
- Bannert, D., & Raza, H. A. (1992). The segmentation of the Indo-Pakistan plate. *Pakistan Journal of Hydrocarbon Research*, 4(2), 5-18.
- Bannert, D., Cheema, A., Ahmed, A., 1989. Interpretation of LANDSAT-MSS Imagery of the Sulaiman and Kirthar Ranges in Western Pakistan, vol. 83. Hydrocarbon Development Institute Pakistan-BGR: Internal Report, p. 2068.
- Bannert, D., Iqbal, M., & Helmcke, D. (1995). Surface and subsurface evidence for the existence of the Sulaiman Basement Fault of the North Western Indian Plate in Pakistan. In *Abstract of the Second South Asia Geological Congress*, Colombo.
- Bensted, J. (1978). δ -dicalcium silicate and its hydraulicity. *Cement and Concrete Research*, 8(1), 73-76.
- Bilqees, R., Sarwar, M. R., Haneef, M., & Khan, T. (2015). Source of cement raw material for the construction of Bhasha Dam in Gilgit Diamir District, Pakistan. *Journal of Himalayan Earth Science*, 48(1).
- Bilqees, R., Tahirkheli, T., Pirzada, N., & Abbas, S. M. (2012). Industrial applications of Abbottabad limestone; utilizing its chemical and engineering properties. *Journal of Himalayan Earth Sciences*, 45(1), 91.
- Brand, N. W., & Brand, C. J. (2014). Performance comparison of portable XRF instruments.
- BS 812-105.2 (1990). Testing aggregates. Methods for determination of particle shape. Elongation index of coarse aggregate (British standard). British Standards Institution, London, United Kingdom.

- BS-812-105.1 (1989). Testing aggregates. Methods for determination of particle shape flakiness index. British Standards Institution, London, United Kingdom.
- BS-812-110. (1990). Testing aggregates methods for determination of aggregate crushing value (ACV). British Standards Institution, London, United Kingdom.
- BS-812-112. (1990). Testing aggregates method for determination of aggregate impact value (AIV). British Standards Institution, London, United Kingdom.
- Craigie, N. (2018). Principles of elemental chemostratigraphy. *Advances in Oil and Gas Exploration & Production*, Rudy Swennen. A Practical User Guide. p189. DOI: <https://doi.org/10.1007/978-3-319-71216-1>.
- Dahl, T. W., Ruhl, M., Hammarlund, E. U., Canfield, D. E., Rosing, M. T., & Bjerrum, C. J. (2013). Tracing euxinia by molybdenum concentrations in sediments using handheld X-ray fluorescence spectroscopy (HHXRF). *Chemical geology*, 360, 241-251.
- Ferraris, C. F., & Ferraris, C. F. (1995). Alkali-silica reaction and high performance concrete.
- Davies L.M. 1941. Correlation of Laki beds. *Geol. Mag.* Vol. 78, 151-152
- French, W. J. (1991). Concrete petrography: a review. *Quarterly Journal of Engineering Geology*, 24(1), 17-48.
- Galetakis, M., Alevizos, G., & Leventakis, K. (2012). Evaluation of fine limestone quarry by-products, for the production of building elements—An experimental approach. *Construction and building materials*, 26(1), 122-130.
- Hemphill, W. R., & Kidwai, A. H. (1973). Stratigraphy of the Bannu and Dera Ismail Khan areas, Pakistan (No. 716-B).
- Humayon, M., Lillie, R. J., & Lawrence, R. D. (1991). Structural interpretation of the eastern Sulaiman foldbelt and foredeep, Pakistan. *Tectonics*, 10(2), 299-324.
- HUSAIN, V., BILQEES, R., & NASREEN, S. (1989). Petrology and industrial application of Nizampur Limestones, NWFP, Pakistan. *Pakistan Journal of Scientific and Industrial Research*, 32(11), 775-779.
- Insley, H. *Microscopy of Ceramics and Cements*; Academic Press, Inc.: New York, NY, USA, 1950

- IQBAL, M. A., & SHAH, S. I. (1980). A guide to the stratigraphy of Pakistan.
- Iqbal, M., Chaudhry, M. N., & Bannert, D. (2008). Hydrocarbon Exploration Concepts for the Eastern Frontal part of Sulaiman Fold Belt. In Pakistan: Society of Petroleum Engineers (SPE)/Pakistan Association of Petroleum Geoscientists (PAPG) Annual Technical Conference, Islamabad, Pakistan.
- Irfan, T. Y. (1996). Mineralogy, fabric properties and classification of weathered granites in Hong Kong. *Quarterly Journal of Engineering Geology and Hydrogeology*, 29(1), 5-35.
- Janjuhah, H. T., Alansari, A., & Vintaned, J. A. G. (2019). Quantification of microporosity and its effect on permeability and acoustic velocity in Miocene carbonates, Central Luconia, offshore Sarawak, Malaysia. *Journal of Petroleum Science and Engineering*, 175, 108-119.
- Janjuhah, H. T., Kontakiotis, G., Wahid, A., Khan, D. M., Zarkogiannis, S. D., & Antonarakou, A. (2021). Integrated porosity classification and quantification scheme for enhanced carbonate reservoir quality: Implications from the miocene malaysian carbonates. *Journal of Marine Science and Engineering*, 9(12), 1410.
- Kadri, I. B. (1995). *Petroleum geology of Pakistan*. Pakistan Petroleum Limited.
- Kazmi, A. H., & Jan, M. Q. (1997). *Geology and tectonics of Pakistan*. (No Title).
- Kemal, A. (1991). Geology and new trends for petroleum exploration in Pakistan. *PAPG Bulletin*, 16-57.
- Khan, M. A., Ahmed, R., Raza, H. A., & Kemal, A. (1986). Geology of petroleum in Kohat-Potwar depression, Pakistan. *AAPG bulletin*, 70(4), 396-414.
- Khanlari, G. R., & Naseri, F. (2018). Prediction of aggregate modified index (AMI) using geomechanical properties of limestones. *Bulletin of Engineering Geology and the Environment*, 77, 803-814.
- Khosa, M. H., Malkani, M. S., Ali, A. M., Hussain, U., Dhanotr, M. S. I., Arif, S. J., ... & Dasti, N. (2016). Stratigraphy, vertebrate paleontology and economic significance of Zinda Pir anticline, Dera Ghazi Khan District, South Punjab, Pakistan. Abstract Volume, Earth Sciences Pakistan 2016, 15-17 July, Baragali Summer Campus, University of Peshawar, Pakistan. *Journal of Himalayan Earth Sciences*, 91.
- Knauth, L. P. (1979). A model for the origin of chert in limestone. *Geology*, 7(6), 274-277.

- López-Buendía, A. M., Climent, V., & Verdú, P. (2006). Lithological influence of aggregate in the alkali-carbonate reaction. *Cement and concrete research*, 36(8), 1490-1500.
- Monnin, Y., Dégrugilliers, P., Bulteel, D., & Garcia-Diaz, E. (2006). Petrography study of two siliceous limestones submitted to alkali-silica reaction. *Cement and concrete research*, 36(8), 1460-1466.
- Nance, H. S., & Rowe, H. (2015). Eustatic controls on stratigraphy, chemostratigraphy, and water mass evolution preserved in a Lower Permian mudrock succession, Delaware Basin, west Texas, USA. *Interpretation*, 3(1), SH11-SH25.
- Nazeer, A., Solangi, S. H., Brohi, I. A., Usmani, P., Napar, L. D., Jahangir, M., ... & Ali, S. M. (2013). Hydrocarbon potential of Zinda Pir anticline, eastern Sulaiman fold belt, middle Indus Basin, Pakistan. *Pakistan Journal of Hydrocarbon Research*, 23, 73-84.
- NIZAMI, A. R. (2008). Sedimentology of the middle Jurassic Samana Suk Formation in Trans Indus Ranges Pakistan (Doctoral dissertation, University of Punjab, Lahore).
- Noor, S. O. H. A. I. L., & Younas, M. U. H. A. M. M. A. D. (2009). Study of limestone from Nizampur area for industrial utilization. *J Chem Soc Pak*, 31(1), 1-5.
- Oates, J. A. (2008). *Lime and limestone: chemistry and technology, production and uses*. John Wiley & Sons.
- Peresson, H., & Daud, F. (2009, November). Integrating Structural Geology and GIS: Wrench tectonics and exploration potential in the eastern Sulaiman fold belt. In *Proceedings, Pakistan Association of Petroleum Geoscientists (PAPG)/Society of Petroleum Engineers (SPE) Annual Technical Conference, Islamabad, Pakistan, November 17th to 18th*.
- Quye-Sawyer, J., Vandeginste, V., & Johnston, K. J. (2015). Application of handheld energy-dispersive X-ray fluorescence spectrometry to carbonate studies: opportunities and challenges. *Journal of Analytical Atomic Spectrometry*, 30(7), 1490-1499.
- Raza, H. A., Ahmed, R., Ali, S. M., & Ahmad, J. (1989). Petroleum prospects: Sulaiman sub-basin, Pakistan. *Pakistan Journal of Hydrocarbon Research*, 1(2), 21-56.

- Raza, H. A., Ahmed, W., Ali, S. M., Mujtaba, M., Alam, S., Shafeeq, M., ... & Riaz, N. (2008). Hydrocarbon prospects of Punjab platform Pakistan, with special reference to Bikaner-Nagaur Basin of India. *Pakistan Journal of Hydrocarbon Research*, 18, 1-33.
- Raza, S. M., Khan, S. H., Karim, T., & Ali, M. (2001). *Stratigraphic Chart of Pakistan*, published by Geological Survey of Pakistan.
- Rehman, S. U. (2009). Microfacies and depositional environments of Kawagarh Formation exposed at Chinali and Kharijala, northwest Lesser Himalaya, Pakistan. Unpublished M. Phil thesis, University of the Punjab, Lahore, Pakistan, 97p.
- Rehman, S. U. (2017). Sedimentology of Turonian-Maastrichtian Kawagarh Formation, Attock Hazara fold and Thrust belt, Northwestern Lesser Himalayas, Pakistan (Doctoral dissertation, University of Sargodha, Sargodha.).
- Rehman, S. U., Ahmed, M., Hasan, F., Hassan, S., Rehman, F., & Ullah, M. F. (2018). Aggregate suitability studies of Middle Jurassic Samana Suk Formation exposed at Sheikh Budin Hill, Marwat Range, Pakistan. *J. Biodivers. Environ. Sci*, 12, 159-168.
- Roberts, F. L., Kandhal, P. S., Brown, E. R., Lee, D. Y., & Kennedy, T. W. (1991). Hot mix asphalt materials, mixture design and construction.
- Rowe, H., Hughes, N., & Robinson, K. (2012). The quantification and application of handheld energy-dispersive x-ray fluorescence (ED-XRF) in mudrock chemostratigraphy and geochemistry. *Chemical geology*, 324, 122-131..
- Sanaullah, M., Khurshid, H. A., Zeeshan, M., Zafar, T., & Zaman, N. (2017). Alkali carbonate reaction (ACR) susceptibility investigations for dolomite of early cambrian by physio-mineralogical techniques. In *International conference on mining and fuel industries (CMFI) October* (pp. 19-21).
- Shah, S. M. I. (1980). *Stratigraphy and economic geology of Central Salt Range*.
- Shah, S. M. I. (2009). *Stratigraphy of Pakistan (memoirs of the geological survey of Pakistan)*. The Geological Survey of Pakistan, 22, 93-114.

- Somro, N., Malkani, M. S., & Zafar, T. (2016, July). Evaluation of Kunhar River aggregate as a construction material, District Mansehra Khyber Pakhtunkhwa, Pakistan. In International conference on: earth sciences Pakistan (pp. 15-17).
- Soulsby, A. G., and A. Kemal, 1988, Review of exploration activity in Pakistan-II: Oil and Gas Journal, v.86, no.48.
- Turner, B. W., Tréanton, J. A., & Slatt, R. M. (2016). The use of chemostratigraphy to refine ambiguous sequence stratigraphic correlations in marine mudrocks. An example from the Woodford Shale, Oklahoma, USA. *Journal of the Geological Society*, 173(5), 854-868.
- Varghese, P. C. (2015). Building materials. PHI Learning Pvt. Ltd.
- Wiersma (1990) Wiersma, M., 1990. The geology of carbonate rocks. In: *Proceeding of International Lime Congress, Rome, Italy*, 51-55"
- Yassin, M. A., Hariri, M. M., Abdullatif, O. M., Makkawi, M., Bertotti, G., & Kaminski, M. A. (2018). Sedimentologic and reservoir characteristics under a tectono-sequence stratigraphic framework: A case study from the Early Cretaceous, upper Abu Gabra sandstones, Sufyan Sub-basin, Muglad Basin, Sudan. *Journal of African Earth Sciences*, 142, 22-43.

APPENDIX

Formula

1. Specific gravity and water absorption

a) Specific Gravity

Oven dry specific gravity (OD) = $A/B-C$

Saturated surface dry specific gravity (SSD) = $B/B-C$ Apparent

specific gravity = $A/A-C$

A= weight of oven dry sample
B= weight of SSD samples
C= weight of sample in water

b) Water absorption

Water absorption % = $(B-A)/A * 100$
A= weight of oven dry sample

B= weight of SSD sample

2. Loss Angeles Abrasion Value (LAAV)

The percent loss was calculated by following formula
LAAV%

= $(W1-W2) / W1 * 100$

W1 = Initial weight

W2 = Weight retained on Sieve No.12 after revolution

3. Aggregate impact value

For each test portion the total mass of fine passing the 2.36 Sieve (MF) to the nearest 0.1 g from.

AVI = $(Mf / Mt) * 100$

Where:

$Mf = Mt - Mr$

Mt= mass of the test portion before testing (g)

Mr= mass of retained on 2.36 mm sieve after testing (g)

4. Aggregate Crushing value (ACU) Aggregate

crushing value = $W_2/W_1 * 100$ Where:

W_1 = total weight of dry sample

W_2 = weight of the portion of crushed material passing 2.36 mm sieve

Appendices No.1 Alkali Silica Reaction Report from Pakistan Council of Scientific & Industrial Research Laboratories Complex, Peshawar



GOVERNMENT OF PAKISTAN
Ministry of Science & Technology
Pakistan Council of Scientific & Industrial Research
Laboratories Complex, Peshawar
Jamrud Road Peshawar 25120-Pakistan

Doc. #PLC/LO/F7/801 Issue Date: 12-12-2022 Rev # 01

Test Report

Page 01 of 01

Test Report # 1050 Lab. Code No. PLC/MSC/515/2023 Date: 21.07.2023
 Case # ILS /ATR/1050/2023
 1. Name & Address of Customer: Mr. Danish Farooq, Islamabad
 Ref No: Nil Dated: 20-06-2023 Date of receipt: 20-06-2023
 2. Description of the Sample (s): Lime Stone Mark if any: N.A
 Item: Lime Stone (01)
 Condition found on receipt: N.A
 3. Sampling Plan/Procedure used: N.A
 4. Environmental Conditions: Temp: 20°C Humidity: 60%
 5. Method Used/Statement of Compliance: ASTM: C 1260
 6. Measurements & Results:

Test of Lime Stone

Parameter	Result
Alkali Silica Reactivity test by accelerated mortar bar method	Expansion less than 0.1% indicating Innocuous nature

7. Remarks/Comments (where required): N.A

- This test/calibration certificate is based solely on the particular sample(s) supplied by the client and should not be reported in part
- Sampling has not been performed by the PCSIR Labs and PCSIR does not accept the responsibility that the item(s) supplied is/are truly representative item(s) of any batch or stock or entire production.
- While the PCSIR agrees to take every reasonable precaution to ensure validity of its test results, it assumes no liability there of beyond the amount of the fee charge for the analysis/test.
- The party shall assume fully responsibility for the ethical use of the results in the test calibration certificate and the laboratory shall be held free from any and all claims, which may result from the use of such data by the client or other.
- After completion of the test/calibration the sample, if required, will be retained for one month until negotiated otherwise.
- The contents, of this certificate cannot be, in any manner, used for the publicity of the product or any advertisement
- Uncertainty of measurements can be provided on request



Reviewed by:

Section Incharge

Verified by:

Head of Centre

Approved by:

Director (P&D)
Director (P&D)

Tel: +92 9221432, PABX No. +92 91 9221398-400, Fax: +92 91 9221398-400
 E-mail: plepesir@gmail.com, Website: www.pcsir-psh.gov.pk